

A UNITED STATES  
DEPARTMENT OF  
COMMERCE  
PUBLICATION

National Bureau of Standards  
Library, E-01 Admin. Bldg.

NOV 7 1969

**NBS TECHNICAL NOTE 381**



# Some Applications of the Josephson Effect

**U.S. DEPARTMENT OF COMMERCE  
NATIONAL BUREAU OF STANDARDS**

# NATIONAL BUREAU OF STANDARDS

The National Bureau of Standards<sup>1</sup> was established by an act of Congress March 3, 1901. Today, in addition to serving as the Nation's central measurement laboratory, the Bureau is a principal focal point in the Federal Government for assuring maximum application of the physical and engineering sciences to the advancement of technology in industry and commerce. To this end the Bureau conducts research and provides central national services in four broad program areas. These are: (1) basic measurements and standards, (2) materials measurements and standards, (3) technological measurements and standards, and (4) transfer of technology.

The Bureau comprises the Institute for Basic Standards, the Institute for Materials Research, the Institute for Applied Technology, the Center for Radiation Research, the Center for Computer Sciences and Technology, and the Office for Information Programs.

**THE INSTITUTE FOR BASIC STANDARDS** provides the central basis within the United States of a complete and consistent system of physical measurement; coordinates that system with measurement systems of other nations; and furnishes essential services leading to accurate and uniform physical measurements throughout the Nation's scientific community, industry, and commerce. The Institute consists of an Office of Measurement Services and the following technical divisions:

Applied Mathematics—Electricity—Metrology—Mechanics—Heat—Atomic and Molecular Physics—Radio Physics<sup>2</sup>—Radio Engineering<sup>2</sup>—Time and Frequency<sup>2</sup>—Astrophysics<sup>2</sup>—Cryogenics.<sup>2</sup>

**THE INSTITUTE FOR MATERIALS RESEARCH** conducts materials research leading to improved methods of measurement standards, and data on the properties of well-characterized materials needed by industry, commerce, educational institutions, and Government; develops, produces, and distributes standard reference materials; relates the physical and chemical properties of materials to their behavior and their interaction with their environments; and provides advisory and research services to other Government agencies. The Institute consists of an Office of Standard Reference Materials and the following divisions:

Analytical Chemistry—Polymers—Metallurgy—Inorganic Materials—Physical Chemistry.

**THE INSTITUTE FOR APPLIED TECHNOLOGY** provides technical services to promote the use of available technology and to facilitate technological innovation in industry and Government; cooperates with public and private organizations in the development of technological standards, and test methodologies; and provides advisory and research services for Federal, state, and local government agencies. The Institute consists of the following technical divisions and offices:

Engineering Standards—Weights and Measures—Invention and Innovation—Vehicle Systems Research—Product Evaluation—Building Research—Instrument Shops—Measurement Engineering—Electronic Technology—Technical Analysis.

**THE CENTER FOR RADIATION RESEARCH** engages in research, measurement, and application of radiation to the solution of Bureau mission problems and the problems of other agencies and institutions. The Center consists of the following divisions:

Reactor Radiation—Linac Radiation—Nuclear Radiation—Applied Radiation.

**THE CENTER FOR COMPUTER SCIENCES AND TECHNOLOGY** conducts research and provides technical services designed to aid Government agencies in the selection, acquisition, and effective use of automatic data processing equipment; and serves as the principal focus for the development of Federal standards for automatic data processing equipment, techniques, and computer languages. The Center consists of the following offices and divisions:

Information Processing Standards—Computer Information—Computer Services—Systems Development—Information Processing Technology.

**THE OFFICE FOR INFORMATION PROGRAMS** promotes optimum dissemination and accessibility of scientific information generated within NBS and other agencies of the Federal government; promotes the development of the National Standard Reference Data System and a system of information analysis centers dealing with the broader aspects of the National Measurement System, and provides appropriate services to ensure that the NBS staff has optimum accessibility to the scientific information of the world. The Office consists of the following organizational units:

Office of Standard Reference Data—Clearinghouse for Federal Scientific and Technical Information<sup>3</sup>—Office of Technical Information and Publications—Library—Office of Public Information—Office of International Relations.

<sup>1</sup> Headquarters and Laboratories at Gaithersburg, Maryland, unless otherwise noted; mailing address Washington, D.C. 20234.

<sup>2</sup> Located at Boulder, Colorado 80302.

<sup>3</sup> Located at 5285 Port Royal Road, Springfield, Virginia 22151.

UNITED STATES DEPARTMENT OF COMMERCE  
Maurice H. Stans, Secretary  
NATIONAL BUREAU OF STANDARDS • Lewis M. Branscomb, Director



## TECHNICAL NOTE 381

ISSUED OCTOBER 1969

Nat. Bur. Stand. (U.S.), Tech. Note 381, 63 pages (Oct. 1969)  
CODEN: NBTNA

### Some Applications of the Josephson Effect

R. A. Kamper, L. O. Mullen, and D. B. Sullivan

Cryogenics Division  
Institute for Basic Standards  
National Bureau of Standards  
Boulder, Colorado 80302

Final Report on Interagency Order NASA-C-7756-B  
National Aeronautics and Space Administration  
Lewis Research Center  
Cleveland, Ohio

NBS Technical Notes are designed to supplement the Bureau's regular publications program. They provide a means for making available scientific data that are of transient or limited interest. Technical Notes may be listed or referred to in the open literature



## CONTENTS

	Page
1. Introduction . . . . .	1
2. The Fabrication of Junctions . . . . .	2
2.1 Niobium Films . . . . .	2
2.2 Niobium-Lead Tunnel Junctions . . . . .	5
2.3 The Mechanism of the Process . . . . .	7
2.4 Performance . . . . .	10
3. Noise Thermometry. . . . .	16
3.1 Measurement Schemes . . . . .	20
3.2 Theoretical Limitations. . . . .	21
3.3 Experimental Tests . . . . .	26
4. Possible Contribution of Superconducting Devices to Nuclear Magnetic Resonance Detection. . . . .	31
4.1 Piecemeal Improvements . . . . .	33
4.2 Magnetometry . . . . .	35
4.3 Conclusions . . . . .	37
5. Overall Conclusions. . . . .	38
APPENDIX . . . . .	39
REFERENCES. . . . .	58

## LIST OF FIGURES

	<i>Page</i>
Figure 1. Variation of pressure in the vacuum chamber during warming of the niobium films at a steady rate after exposure to oxygen at a temperature of about 80 K . . . . .	9
Figure 2. Tracing of the current versus voltage characteristic of a niobium-lead Josephson junction prepared by this process . . . . .	11
Figure 3. Constant voltage steps generated by microwave irradiation at 8.34 GHz . . . . .	14
Figure 4. Josephson oscillation of a thin film junction at 38 MHz . . . . .	17
Figure 5. Basic circuit for noise thermometry . . . . .	18
Figure 6. Arrangement for noise thermometry by frequency counting . . . . .	28
Figure 7. Details of junction, bias resistor, and primary of output transformer. The gap between the niobium and brass blocks is exaggerated for clarity . . . . .	30
Figure 8. Current versus voltage characteristic of a thin film Josephson junction . . . . .	42
Figure 9. Dependence of $I_C$ (fig. 8) on applied magnetic field. The scales depend upon the geometry of the junction . . . . .	43
Figure 10. The quantum interferometer, a) ideal, b) early practical version (ref. 47). . . . .	44

LIST OF FIGURES (Continued)

Page

Figure 11.	Current versus voltage characteristic of a thin film Josephson junction connected to a circuit with a resonance at frequency $f = 2eV/h$ . . . . .	46
Figure 12.	Current versus voltage characteristic of a Josephson junction irradiated at a frequency $f = 2eV/h$ . . . . .	47
Figure 13.	Josephson oscillation. The response of a receiver tuned to 43 MHz is displayed as a function of DC bias on the Josephson junction . . . . .	48
Figure 14.	The Clarke null detector . . . . .	50
Figure 15.	The tunneling cryotron . . . . .	52
Figure 16.	Current versus voltage characteristic of the gate of a tunneling cryotron. The operating points are marked A and B. . . . .	53



# SOME APPLICATIONS OF THE JOSEPHSON EFFECT

R. A. Kamper, L. O. Mullen, and D. B. Sullivan

We describe techniques for fabricating permanent Josephson junctions between thin films of niobium and lead, and for absolute noise thermometry at very low temperatures using the Josephson effect. We discuss the possible benefits of applying superconductivity to nuclear magnetic resonance detection, and review other applications of the Josephson effect.

**Key Words:** Josephson effect; superconductivity; tunnel junctions; thermometry.

## 1. Introduction

This is the final report on work performed on Interagency Order NASA-C-7756-B, for the Lewis Research Center of the National Aeronautics and Space Administration, with additional funding from the National Bureau of Standards. It is a sequel to NASA Contractor Report CR 1189 (September, 1968), in which we described our early studies of the Josephson effect and its applications. In that report we described the characteristics of Josephson oscillation which we had observed; methods for fabricating Josephson junctions; and designs for, and early tests of, a picovoltmeter and a noise thermometer for the millikelvin range. We subsequently chose the fabrication of junctions and the noise thermometer for further development, and we report the results of that effort here. We have developed a permanent, rugged tunnel junction between thin films of niobium and lead, with electrical characteristics that show great promise for permanent instruments based on the Josephson effect. We will describe the fabrication and properties of this type of junction in full detail in this report. We have investigated the theoretical limitations of noise thermometry with the Josephson effect, and constructed a practical system for testing in the

millikelvin range. These will also be discussed. An important aspect of the practical application of superconductivity to electronics is the search for opportunities in activities that could benefit from improved instruments. With this in mind, we analyzed the improvement that could be made in nuclear magnetic resonance detection by the application of superconducting devices. We present this analysis in this report. Finally, to fill in the background for our work and to indicate other areas of opportunity, we included as an appendix a review of the Josephson effect and its applications which we prepared for the IEEE Transactions on Instrumentation and Measurement.

## 2. The Fabrication of Junctions

In our previous report<sup>[1]</sup> we described several methods we had tried for fabricating Josephson junctions between thin films of niobium and lead. We have given further attention to the most successful of these methods, as well as the problem of protecting the junctions from deterioration in storage. In this chapter we present the resulting recipe for making junctions which can survive thermal cycling and storage at ambient temperature, exposed to the atmosphere, for many months without measurable deterioration. We also comment on the probable mechanism of the process and on the performance of the junctions.

### 2.1 Niobium Films

We prepare our niobium films by evaporation, at a rate of  $10\text{\AA}$  per second, in a high vacuum ( $\sim 10^{-9}$  Torr, or  $1.3 \times 10^{-7}\text{N/m}^2$ ), onto a sapphire substrate maintained at a temperature of  $400^\circ\text{C}$ .

The vacuum system we use is a large stainless steel chamber equipped with a titanium sublimation pump (with liquid nitrogen cooled pumping surface), a large (135 liter/second) ion pump, and a small roughing system, consisting of a mechanical roughing pump and an oil vapor diffusion pump, connected to the main vacuum chamber via an elaborate cold trap. This last is valved off during high vacuum runs.

The working space is surrounded by coils of tubing through which we circulate liquid nitrogen. Stray niobium vapor condenses on these coils during (and before) deposition of the films, and assists the other pumps by absorbing residual gas.<sup>[2]</sup> We start our runs by thoroughly outgassing all parts of the system near their highest working temperatures.

The evaporation source is a drop of molten niobium, approximately 1 cm diameter, in a water-cooled copper boat. It is heated by electron bombardment from a heated loop of tungsten wire. By means of some carefully placed electrostatic shields, the majority of the electrons are guided to strike the niobium. Stray electrons cause troublesome heating of the parts they strike. A total power of 1.2 kW is sufficient to maintain the niobium at a temperature of 3200 K, measured by optical pyrometry using the melting point of niobium to check the instrument. At this temperature the niobium evaporates at a rate sufficient to deposit 10 Å of niobium film per second on a substrate 25 cm away. We developed this evaporation source by adapting a commercial unit which was unsatisfactory in its original form.

We chose single crystal sapphire substrates for their excellent thermal conductivity at low temperature. For depositing films we have a substrate holder equipped with a movable mask and a shutter, as well as means for raising (with a heater) and lowering (with liquid nitrogen) the temperature, and a thermocouple to measure it. The complete assembly fits in a 3.5 cm port in the side of the vacuum chamber.

We usually evaporate the niobium onto substrates at 400°C. A lower substrate temperature results in films with low superconducting transition temperatures. Neugebauer and Ekvall<sup>[2]</sup> attributed this effect to contamination of the films deposited on cold substrates by residual gases in the vacuum system. They suggested that contamination

is favored by a low temperature and cited evidence to support this hypothesis. However, it is interesting to note that we obtain similar results to theirs although we have an initial vacuum four orders of magnitude lower in pressure and an evaporation rate one order of magnitude greater. Our films are of better quality (as judged from their superconducting transition temperatures) than they reported, but we have to maintain our substrates at a similar temperature to achieve the best quality. It is possible that variations in the crystal structure of the deposited films with substrate temperature affect the superconducting transition temperature independently of any contamination.

We have observed with a polarizing microscope that even our good films have a non-cubic crystal structure with orientation controlled by the substrate.

The superconducting transition temperatures we observe depend upon film thickness, being depressed below the value for bulk niobium in films less than  $1000\text{\AA}$  thick. The following table shows the relationship between film thickness and transition temperature for a reasonably good set of films.

Film Thickness ( $\text{\AA}$ )	Transition Temperature (K)
11000	9.2
2200	9.3
1300	8.9
600	8.7
300	7.9
200	6.9

The transition temperature of bulk niobium lies somewhere between  $9.19\text{ K}$ <sup>[3]</sup> and  $9.46\text{ K}$ <sup>[4]</sup>.

These films have a mirror-like appearance, even under a microscope with a magnification of a few hundred diameters. They are attached very firmly to their substrates, and survive soldering of leads, thermal cycling to low temperatures, abrasion, careless handling, atmospheric corrosion, etc. They may be removed with hydrofluoric acid, to which the sapphire substrates are resistant.

In response to a request from the NASA-Lewis Research Center, we found a technique for separating a niobium film intact from its substrate. We started by evaporating a layer of copper, about  $2000\text{\AA}$  thick, on a sapphire substrate at ambient temperature. We then heated it to  $400^\circ\text{C}$  and deposited a film of niobium about  $1000\text{\AA}$  thick. After cooling this structure and removing it from the vacuum chamber, we slowly immersed it in a 10% solution of nitric acid. Most of the copper dissolved in the acid and the niobium film floated off intact. We collected it on a perforated metal plate and rinsed it with water containing some ethyl alcohol to reduce the surface tension, which would otherwise break the film.

## 2.2 Niobium-Lead Tunnel Junctions

In brief, we make our tunnel junctions by exposing cold (80 K) niobium films to a glow discharge in oxygen, driving off unwanted discharge products with a thermal cycle, and depositing the lead films over the treated niobium films.

After depositing the niobium films we cool the substrates to about 80 K by circulating liquid nitrogen in the substrate holder. We normally maintain this temperature for about one hour before proceeding with the next stage. Then, we shut down the pumps and admit oxygen at a pressure between  $5 \times 10^{-3}$  Torr and  $2 \times 10^{-2}$  Torr (0.7 to  $3 \text{ N/m}^2$ ). We maintain a glow discharge in the oxygen gas at 300 V

and about 200 mA for a period varying from 200 sec to 220 sec, using the chamber wall and substrate holder for the negative electrode. We find that the addition of about 10% nitrogen to the oxygen facilitates control of the discharge.

The exposure time is critical. If it is too short continuous barriers fail to form. Too long an exposure generates a visible frost which disappears during the subsequent thermal cycling, and the quality of the junctions then depends very strongly on the temperature reached during the thermal cycle, making quality control very difficult.

After exposure of the niobium films to the discharge, we restart the pumps to restore the vacuum. We then heat the niobium films, with an electric heater in the substrate holder, up to a temperature between -50°C and -80°C, measured with a thermocouple. If the films have been overexposed to the discharge, they can be restored to a usable condition at this stage by continuing the heating to a higher temperature. As soon as the films reach the peak temperature, we cool them to 80 K by circulating liquid nitrogen, and deposit the lead films by evaporation from a source similar to the one we use for niobium. Before removing the junctions from the vacuum we warm them up to ambient temperature in order to avoid condensing water on them, which attacks the lead films.

Finally, to protect the lead films from atmospheric corrosion, we coat the junctions with polyimide plastic. We heat them to about 100°C in air to dry them thoroughly, and paint on a thin layer of the unpolymerized plastic thinned 10:1 with a thinner provided by the manufacturer. Both the warming and the thinning of the plastic are necessary precautions to avoid destroying the junctions.

We normally attach leads to the films by a soldering technique invented by Dr. V. D. Arp, of this laboratory. First, we cover the area of film to be soldered with a thin layer of either an air drying varnish or polyimide plastic. When this layer is hard, we solder the leads on with indium. No flux is necessary. The molten indium appears to melt the varnish, forming a good mechanical bond with satisfactory electrical contact. Some care must be taken with lead films because the indium dissolves the lead. This problem does not arise with niobium, and we try to arrange our evaporation masks so that we deposit patches of niobium film under the parts of the lead films where we intend to solder leads.

### 2.3 The Mechanism of the Process

We believe that the barriers in our niobium-lead tunnel junctions are formed by some active product of the glow discharge, which condenses on the cold niobium films and remains there as an adsorbed layer which then attacks the lead film after its deposition, forming a barrier of some compound of lead.

The main evidence in support of this hypothesis comes from the effects of variations in the process. If we use rather a long exposure of the cold niobium films to the glow discharge, and omit the subsequent thermal cycle before depositing the lead, the lead film is completely destroyed on warming, leaving a transparent dielectric layer overlapping the intact niobium film. If we use a normal exposure, and extend the thermal cycle up to ambient temperature before depositing the lead, the result is a simple metallic contact between the niobium and lead films. In contrast, we can heat the complete niobium-lead junctions up to at least 150°C with impunity. These two observations suggest strongly that it is the lead alone which reacts to form the barrier. An

additional piece of evidence is that the process is very specific. We have been unable to make niobium-magnesium tunnel junctions at all this way, and niobium-aluminum junctions have all been of inferior quality.

The big unanswered question is the identity of the active species which condenses on the cold niobium films and subsequently attacks the lead. In this connection we call attention to figure 1, which shows the variation of pressure in the vacuum chamber with temperature as the substrates and niobium films are warmed at a steady rate from 80 K to ambient temperature. Two curves are shown. The upper curve corresponds to our normal routine for making tunnel junctions using a glow discharge. The lower curve was observed after exposure to oxygen in the absence of a glow discharge. The pressure of oxygen during exposure is indicated by the symbol  $\Delta P(O_2)$ .

The most striking features of figure 1 are the multiple peaks of pressure and the wide difference between the two curves. The weak presence of the main peaks in the lower curve may be due to the ion pump, which was running continuously while these curves were being recorded. It appears that the discharge generates several species of low vapor pressure which condense on the cold surfaces and then evaporate at different temperatures. An analysis of the composition of the gas in the vacuum system with a mass spectrograph confirms this impression. We observe prominent components of the mass spectrogram corresponding to 11 distinct molecular species, all of which contribute to the first large peak in pressure shown in figure 1.

The top six components of that peak (in order of intensity) have mass/charge ratios: 44(CO<sub>2</sub>); 28(CO, N<sub>2</sub>); 16(CH<sub>4</sub>, O); 40(A); 12, 13(C); 18(H<sub>2</sub>O). The numbers are in atomic units and the most likely chemical assignments are given in parentheses. The ratio of concentrations

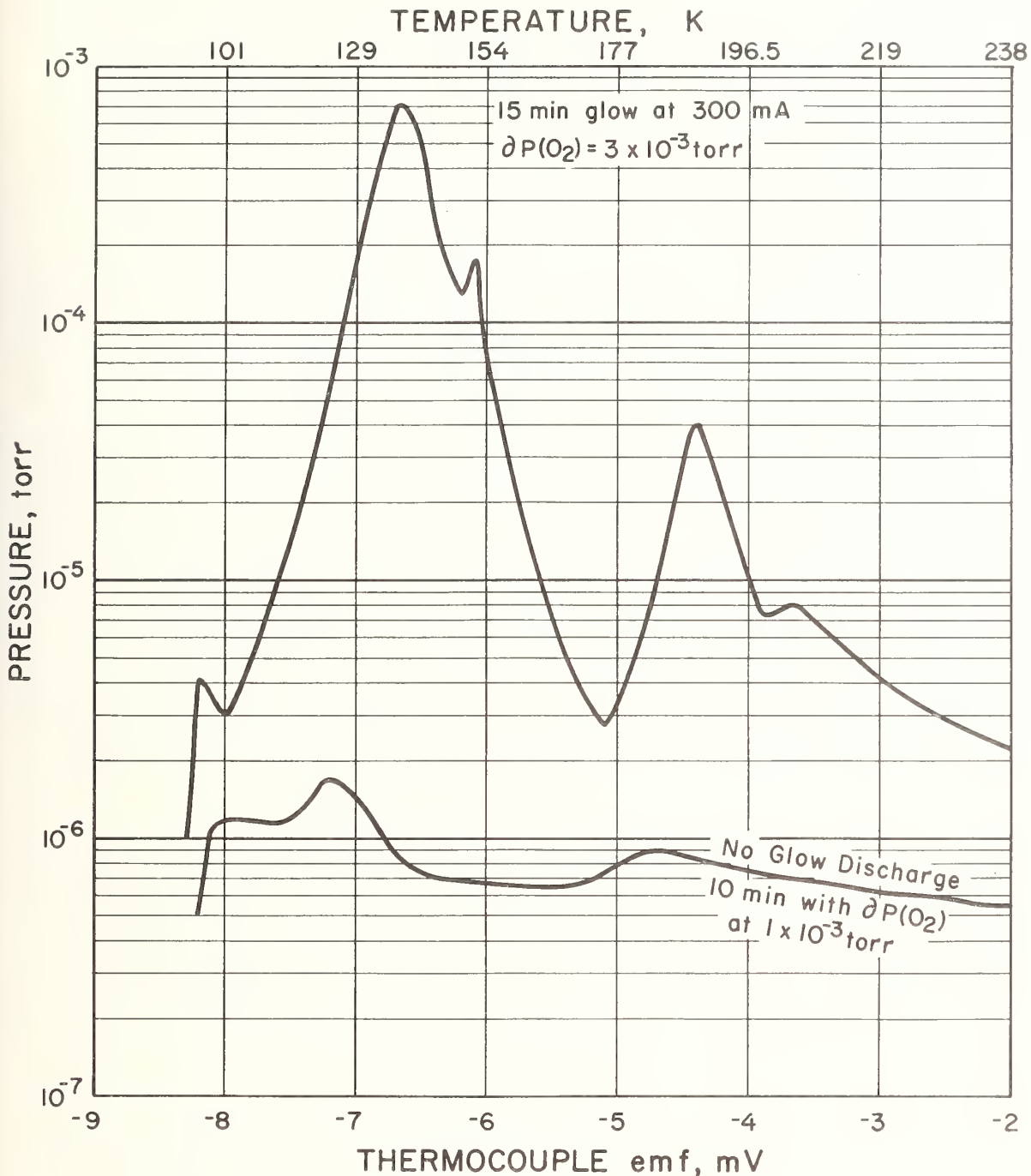


Figure 1. Variation of pressure in the vacuum chamber during warming of the niobium films at a steady rate after exposure to oxygen at a temperature of about 80 K.

of the two isotopes of carbon corresponds to their natural relative abundance. Together, these six species account for 95% of that first large peak in figure 1. The second prominent peak in figure 1 contains contributions from: 18(H<sub>2</sub>O) and 28(CO, N<sub>2</sub>), which account for 70% of the total pressure. Other minor constituents are: 15(CH<sub>3</sub>), 17(OH), 14(N), 29(?), 30(NO). In addition, there are faint traces of: 48(O<sub>3</sub>); 46(NO<sub>2</sub>); 44(N<sub>2</sub>O); 38, 36(HCl); 37, 35(Cl). These last are very reactive gases which may have an influence out of proportion to their concentration.

Many of the more volatile molecular species we have listed may have been trapped by less volatile components, such as carbon dioxide, or generated by decomposition of more complex molecules by ion bombardment within the mass spectrograph. The presence of carbon, hydrogen, argon, and chlorine in the vacuum chamber must be due either to impurities in the oxygen or to release from the chamber walls by the action of the glow discharge. It would be possible to eliminate them in a bakeable system.

The most likely candidate for the active agent that attacks the lead films appears to be water. However, we have tried exposing the niobium films to water vapor without a glow discharge and did not succeed in producing adequate barriers. The direct action of the glow discharge appears to be essential.

#### 2.4 Performance

A common characteristic of junctions fabricated by the technique discussed in this chapter is their freedom from background current due to processes other than quantum mechanical tunneling. A tracing of a typical current vs. voltage characteristic of one of our junctions at 4 K is shown in figure 2. The current that passes at zero voltage depends

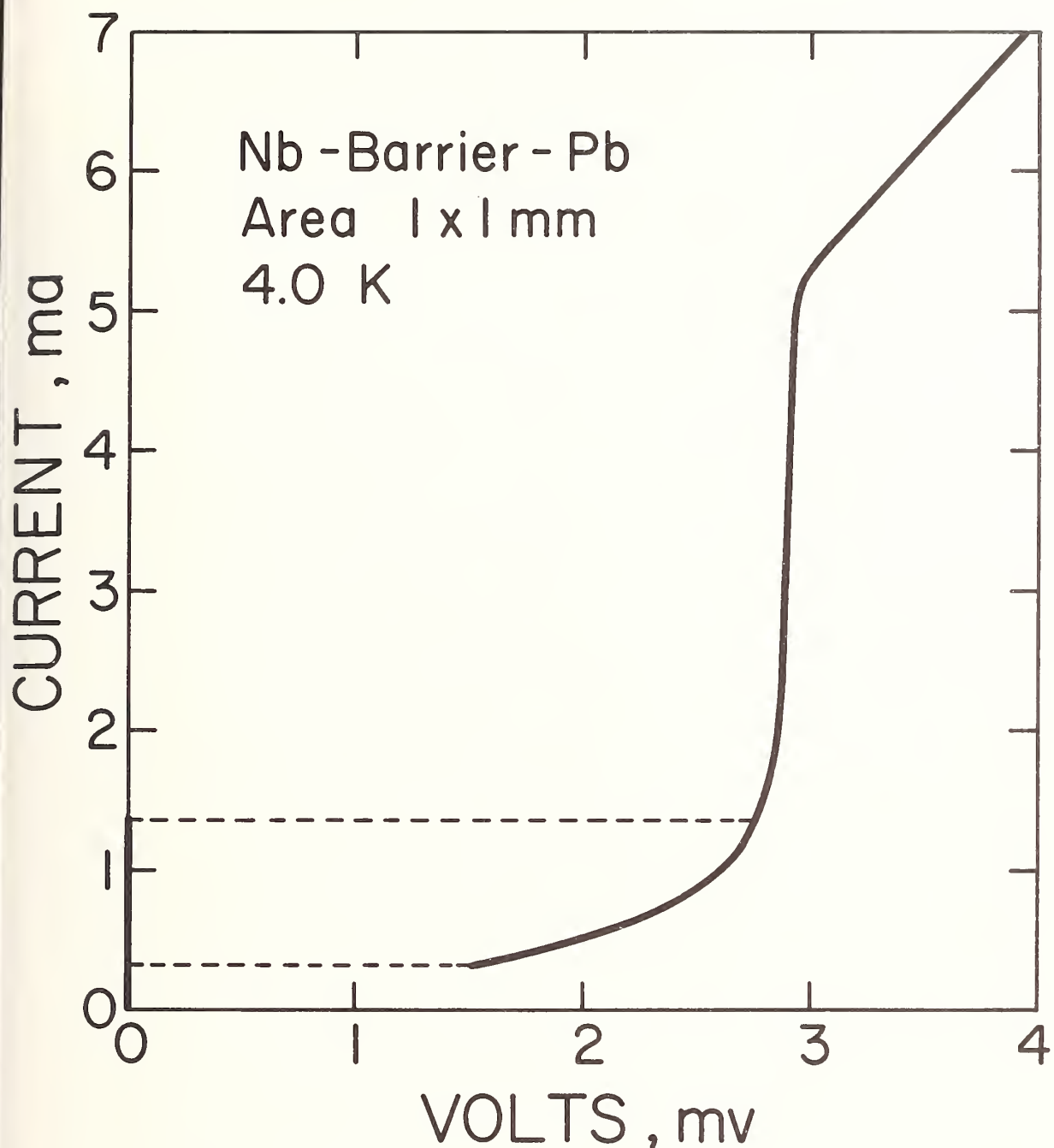


Figure 2. Tracing of the current versus voltage characteristic of a niobium-lead Josephson junction prepared by this process.

very strongly on the orientation of the junction in the Earth's magnetic field, indicating that it is a true Josephson tunnel current. The part of the curve at small but finite voltage can be explored either by suppressing the Josephson current with a magnetic field, or by decreasing the current from a value exceeding the maximum Josephson current. It shows typical quasi-particle tunneling behavior, with a sharp rise near 3 mV associated with the energy gaps of the superconductors, followed by an ohmic response to higher voltage.

We regard a junction as acceptable if the (ohmic) background current is less than 10% of the tunnel current in the ohmic region of the curve. The yield of acceptable junctions is about 60% if we include failures due to obvious causes such as vacuum leaks, malfunction of pumps, etc. Counting only runs in which we adhere to the specified conditions, the yield is near 100%. However, it has proven difficult to control the resistance of the junctions, which is a measure of the barrier thickness. We have made acceptable junctions with resistances varying from  $0.06\Omega$  to  $10\Omega$  (for a junction  $1\frac{1}{4}$  square), measured at 4K in the ohmic range above 3 mV. In general, only junctions with resistance less than about  $1\Omega$  show a Josephson current. Part of the problem is caused by poor thermal contact between the sapphire substrates and the substrate holder. We notice that junctions sharing a substrate usually have very similar resistance, which differs from that of junctions on other substrates made in the same run. A solution to this problem which we are working on is to take advantage of the longevity of these junctions and build up a library of junctions with graded characteristics.

Sets of these coated junctions have survived the following endurance tests, with no detectable deterioration:

1) Storage at ambient temperature, exposed to the atmosphere, for a period of 4 months. This indicates that the junctions are stable against diffusion into the films.

2) 400 dips into liquid nitrogen, allowing time for the junctions to warm up to ambient temperature, while exposed to the atmosphere, between dips. The frost that forms during this treatment would rapidly destroy unprotected lead films.

3) Soldering leads on with indium 3 or 4 times.

In test (2) the leads were detached by differential thermal contraction after an average of 50 dips. However, on replacing the leads we found no detectable deterioration of the junctions. In test (3) there was a tendency to destroy the lead films by dissolving them in indium, but the junctions remained intact.

We emphasize that we have not yet tested any of these coated junctions to destruction. They were all usable after these tests, which must continue to find the limits of abuse they will survive. However, they have already demonstrated great promise for application in permanent instruments.

We have observed the expected effect of irradiation, with microwaves at X-band, on the DC characteristics of these junctions (see appendix). Figure 3 shows a recorder trace of the direct current vs. voltage characteristic demonstrating constant voltage steps at interval  $V = hf/2e$ , where  $h$  is Planck's constant,  $f$  is the microwave frequency, and  $e$  is the electron charge. We also sent a junction to Dr. H. A. Fowler, at the National Bureau of Standards in Gaithersburg, who reported that it would be usable for his purpose of determining the fundamental constant  $e/h$  very accurately by relating the voltage interval of the steps to the NBS standard volt.

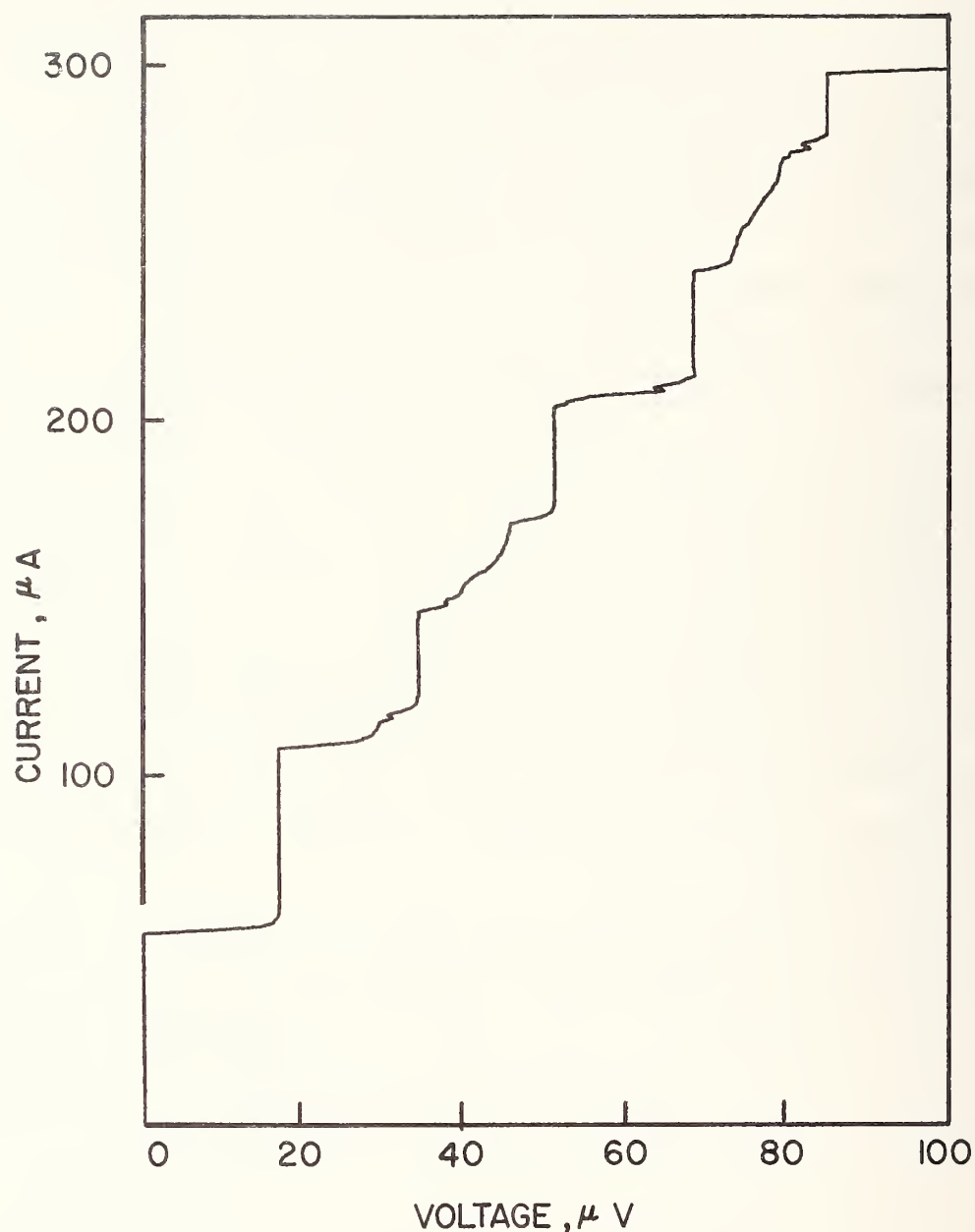


Figure 3. Constant voltage steps generated by microwave irradiation at 8.34 GHz.

We have also observed free oscillation of one of these junctions at 38 MHz, driven by a steady bias voltage of about  $8 \times 10^{-8}$  V. This frequency is more than two orders of magnitude lower than previously observed with thin film junctions.

Generation of oscillation at this frequency requires a very small resistor ( $\sim 10^{-6}$   $\Omega$ ) connected in parallel with the junction in a low inductance circuit to maintain the bias voltage. We therefore used a sapphire substrate in the form of a square, 0.5 cm on each side and  $0.25\frac{1}{4}$  thick. This was placed on one face of a 0.5 cm cube of brass which functioned as the bias resistor. Two opposite faces of the block were coated with lead-tin solder to form superconducting electrodes. The strips of niobium and lead films forming the junction were  $0.2\frac{1}{4}$  wide and about  $1000\text{\AA}$  thick. They were connected to the bias resistor and the tuned output circuit with short lengths ( $\sim 1\frac{1}{4}$ ) of fine tinned copper wire. The junction, bias resistor, and tuned output transformer (for impedance matching) were enclosed in a copper screening can with a single layer solenoid wound outside. This supplied a steady magnetic flux density in the range from zero to one millitesla. The need for this magnetic field precluded the use of superconducting screens and made the junction rather susceptible to noise radiated from outside the cryostat (we did not have a screened enclosure for this work).

The spectrum of oscillations we observed at 38 MHz as we varied the steady bias voltage was a strong and quasi periodic function of applied magnetic field. As we varied the field we could generate one, two, or three quantum transitions, with some regions of field in which the oscillation appeared to be suppressed. The change in flux density required to make a drastic change in the spectrum of oscillations was of the order of 100 microtesla in any part of the available range of  $\pm 1000$  microtesla. It is natural to associate this behavior

with the well known periodic dependence of the DC properties of thin film Josephson junctions on applied magnetic field (see appendix). The period one would expect for a junction with dimensions like ours would indeed be about 100 microtesla. However, the response of the Josephson oscillation to a magnetic field which we observe is rather complex and hysteretic, probably because of trapped magnetic flux in superconducting parts of the apparatus. The frequency at which we were working was much too low to excite the microwave resonances which are present in Josephson junctions by virtue of their low phase velocity for wave propagation.<sup>[5]</sup>

We show a recorder trace of the Josephson oscillation at 38 MHz plotted against DC bias in figure 4. The steady magnetic flux density was about 750 microtesla. The oscillation was nearly sinusoidal. The second harmonic (at  $\frac{1}{2}$  bias voltage) is clearly visible but higher harmonics are almost absent. The line width of the oscillation was somewhat dependent on magnetic field and rather broad, of the order of 1 MHz. This will need to be reduced for practical applications of this oscillation.

### 3. Noise Thermometry

The principle of the application of the Josephson effect to noise thermometry is illustrated in figure 5. The Josephson junction is connected by leads of very small inductance ( $< 10^{-9}$  H) to a shunt of small resistance  $R$  ( $\sim 10^{-5}$   $\Omega$ ). A direct current  $I$  of the order of 10 mA through this shunt will maintain a steady bias voltage of the order of  $10^{-7}$  V across the junction, driving it to oscillate at a frequency of the order of 50 MHz.<sup>[6]</sup> The frequency  $f$  of oscillation is related to the bias voltage  $V$  across the junction by

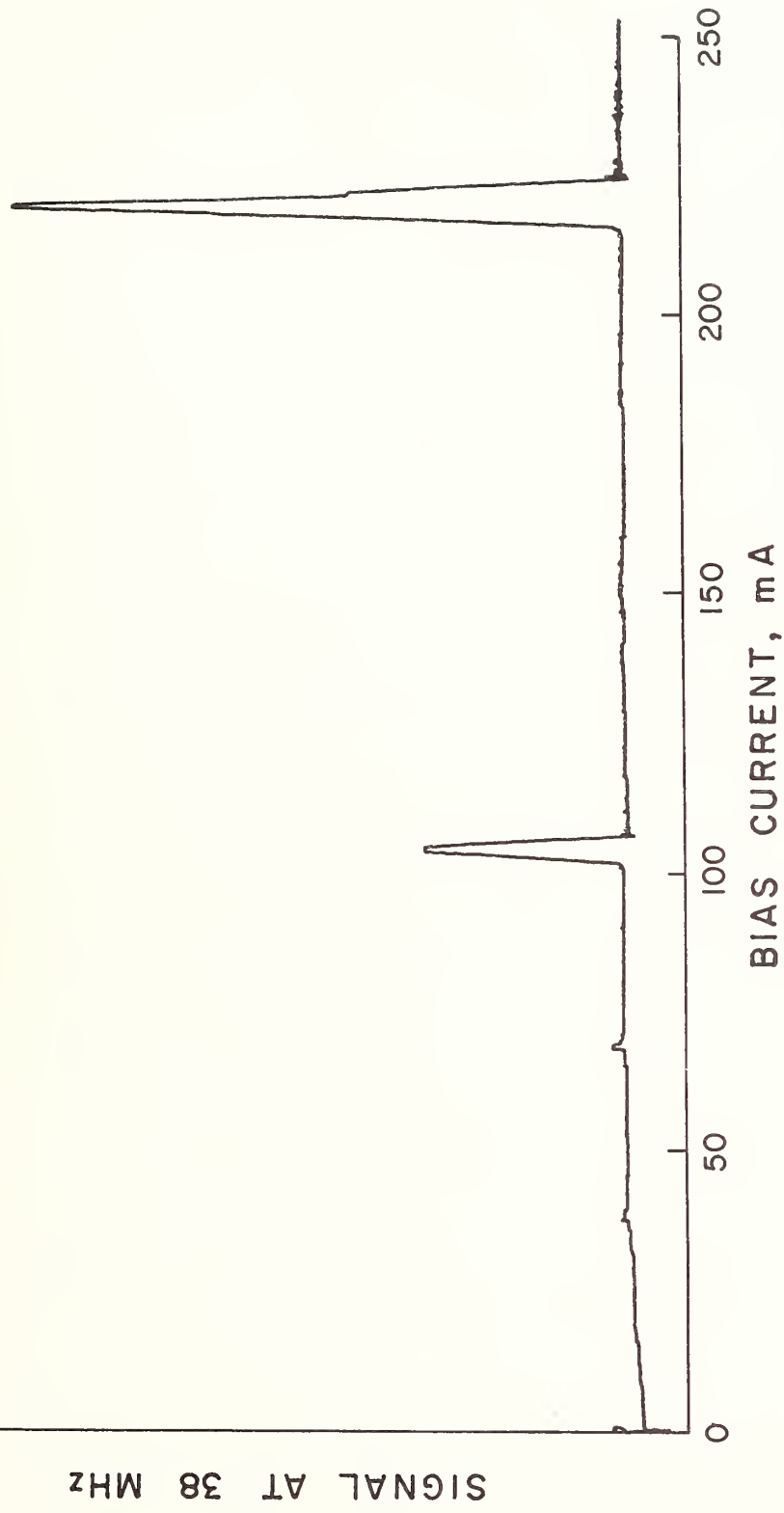


Figure 4. Josephson oscillation of a thin film junction at 38 MHz.

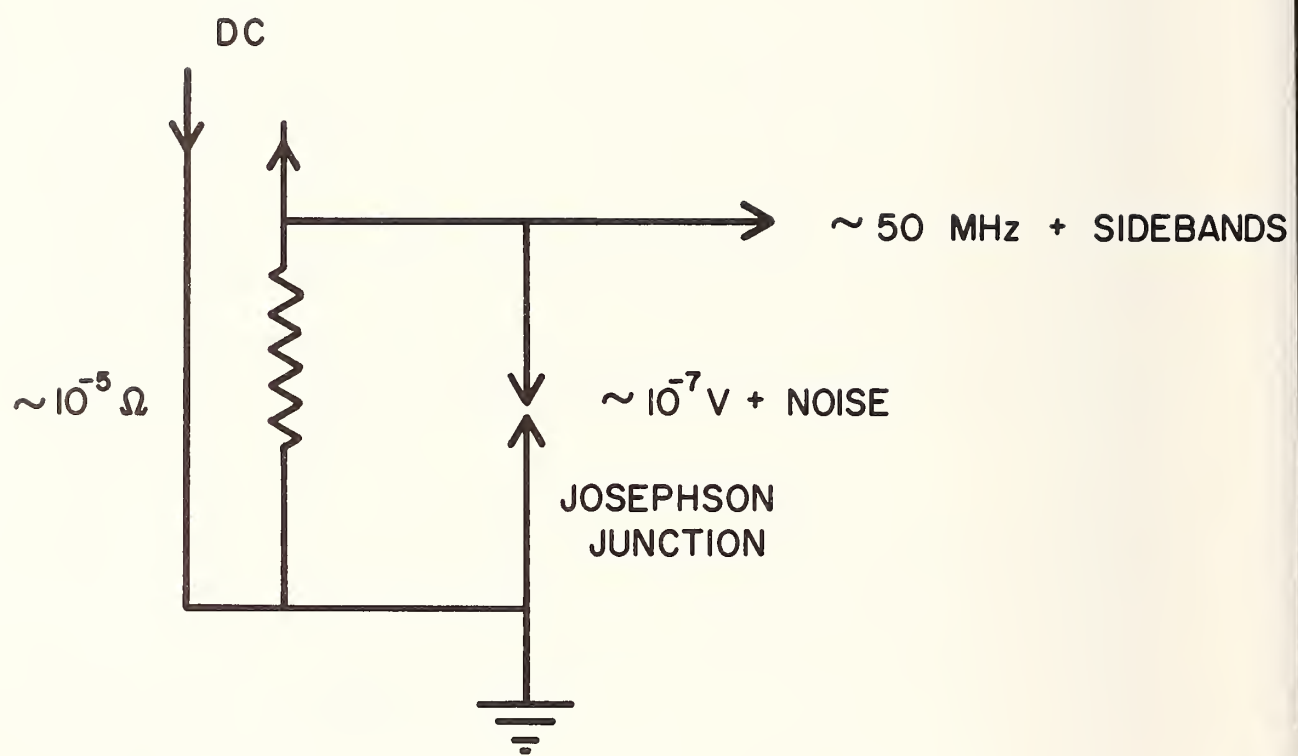


Figure 5. Basic circuit for noise thermometry.

$$hf = 2eV$$

or

$$f = V/\varphi_0 \quad (1)$$

where  $h$  is Planck's constant,  $e$  is the electron charge, and  $\varphi_0 = h/2e$  is the magnetic flux quantum. The voltage  $V$  across the junction is

$$V = IR + \text{noise} \quad (2)$$

and the fluctuations in  $V$  due to noise will be converted into fluctuations in the frequency  $f$ . If the shunt resistance  $R$  is small compared with the resistance of the junction and the impedance of the current supply, its Johnson noise will dominate the fluctuations in the frequency of oscillation. These fluctuations will then contain sufficient information to determine the absolute temperature of the shunt resistor.

In the remainder of this chapter we will describe practical schemes for thermometry based on this principle and discuss their theoretical limitations. It appears to be theoretically possible to measure noise temperatures in the millikelvin range. Finally, we will discuss the performance of prototype thermometers.

The essential components of a noise thermometer are a resistor to generate thermal noise and a preamplifier, with noise temperature less than the temperature to be measured, and with sufficient gain to generate a signal detectable by a receiver at ambient temperature. In the arrangement we describe here the Josephson junction fulfills the function of the preamplifier. A simple analysis<sup>[1, 7]</sup> shows that the components of the noise spectrum which have the greatest effect on the spectrum of the Josephson oscillation are all at low frequency (< 1 kHz at 4 K, less at lower temperatures). They create a narrow spectrum of sidebands close to the center frequency  $IR/\varphi_0$ . Thus the Josephson junction amplifies the noise signal by parametric up-conversion.<sup>[8]</sup> The oscillation of the junction is the pump, the input frequency is less than 1 kHz, and the output (idler) frequency is near the oscillation frequency of 30-

50 MHz. The maximum theoretical power gain of such an amplifier is the ratio of output to input frequencies,<sup>[9]</sup> which is in excess of  $10^4$  at 4 K and may be as much as  $10^7$  at lower temperatures. With this preamplifier an ordinary radiofrequency communications receiver should suffice for noise measurements.

### 3.1 Measurement Schemes

We will discuss two approaches to the measurement of Johnson noise using the Josephson effect, which we will call by the names spectrum analysis and frequency counting.

Spectrum analysis requires a narrow band receiver to explore the long-term average of the spectrum of sidebands near the Josephson oscillation frequency. The quantity measured is the linewidth  $\Delta f$ , which is the frequency interval between the two points at which the spectral density is one half of its peak value at the unperturbed frequency  $IR/\phi_0$ . Assuming that the only significant source of broadening is Johnson noise from the shunt resistor  $R$ , the mean square fluctuation in voltage  $\bar{V}_n^2$  across the junction is given by

$$\bar{V}_n^2 = \int 4kTR \cdot df \quad (3)$$

where  $k$  is Boltzman's constant,  $T$  is the absolute temperature, and  $df$  is an interval of frequency. Application of standard FM theory to the corresponding fluctuation in frequency yields a formula for the observed linewidth  $\Delta f$ :<sup>[10]</sup>

$$\Delta f = 4\pi kTR/\phi_0^2$$

or

$$\Delta f = (4.03 \times 10^7)RT. \quad (4)$$

We will discuss the experimental verification of this formula in section 3.3.

We have given most of our attention to the alternative approach, frequency counting. A signal derived from the Josephson oscillation is amplified and used to drive a frequency counter, which repeatedly counts the number of cycles in a fixed gate time  $\tau$ . Fluctuations in the frequency then appear directly as fluctuations in the count. A convenient measure of these fluctuations is the variance, or mean square deviation  $\sigma^2$ . If the only noise present is white, thermal noise generated by the resistance  $R$ , then

$$\sigma^2 = \overline{(f - \bar{f})^2} = 2kTR/\tau\phi_0^2$$

or

$$\sigma^2 = (6.4 \times 10^6) RT/\tau. \quad (5)$$

This approach to noise measurement has the advantages that it is easy to automate the recording of data and to discriminate against spurious sources of noise, such as flicker noise, with anomalous power spectra.

In both these schemes of thermometry the measured quantity is related to the absolute temperature by an expression containing fundamental constants and easily measured quantities only. In principle no calibration is required.

### 3.2 Theoretical Limitations

In this section we discuss the fundamental theoretical limitations on the range and accuracy of noise thermometry with the Josephson effect.

First, let us discuss the validity of the Nyquist formula, equation (3), on which equations (4) and (5) are based. This formula is based on Boltzmann statistics, whereas the photons involved in the generation of noise should properly be described with Bose statistics. The

difference is only significant at very low temperatures, such that

$$hf \geq kT$$

or

$$f/T \geq 20 \text{ GHz/K.} \quad (6)$$

We have shown<sup>[7]</sup> that the components of the noise spectrum which have the major effect on the Josephson oscillation are those at frequencies of the order of the linewidth  $\Delta f$  (equation 4) or less. A comparison of equation (4) with the limit given in equation (6) shows that Boltzman statistics, and hence the Nyquist formula, should be an excellent approximation at any temperature.

Next we consider the current supply to maintain the constant bias voltage on the shunt resistor  $R$ . In its simplest form this would consist of a battery with an emf of a few volts in series with a resistor  $R_o$ , of the order of  $10^3 \Omega$ , at ambient temperature  $T_o$ . Neglecting the battery, the effective noise temperature  $T_n$  of the combination of  $R$  and  $R_o$  in parallel is

$$T_n = (R T_o + R_o T) / (R + R_o). \quad (7)$$

The contribution to  $T_n$  from the resistor  $R_o$  at ambient temperature is  $R T_o / (R + R_o)$ . If  $R = 10^{-5} \Omega$  and  $R_o = 10^3 \Omega$ , then this amounts to  $3 \times 10^{-6} \text{ K}$ , which is clearly negligible. The question of noise contributed by the battery has been investigated by Knott.<sup>[11]</sup> He tested several different dry cells and found the noise that they generated in the frequency range of interest was comparable with Johnson noise on a resistor of  $10^3 \Omega$  at ambient temperature. Thus the combination of battery and resistor would be a satisfactory power supply for noise thermometry down into the microkelvin range.

The ultimate low temperature limit to the Josephson noise thermometer will most likely be set by the noise temperature of the junction itself. This has been analyzed by several authors,<sup>[12-16]</sup> most completely and recently by Stephen.<sup>[15, 16]</sup> We will summarize his conclusions briefly.

A perfect junction transmits current by tunneling of Cooper pairs and by tunneling of quasi particles. The respective contributions of these two processes to the total current depend upon voltage and temperature. The significant differences so far as noise is concerned are in the quantities  $I/V$ ,  $\partial I/\partial V$ , and the double charge per particle carried by Cooper pairs. At high temperatures, when  $kT \gg eV$ , both processes generate Johnson noise appropriate to the temperature and some suitably defined effective resistance (equation 3). At very low temperatures ( $kT \ll eV$ ) they only generate shot noise. This is similar to Johnson noise at an effective temperature  $T_{eff}$ , where

$$T_{eff} \approx eV/k$$

or

$$T_{eff} \approx hf/2k \quad (8)$$

where  $f$  is the frequency of Josephson oscillation. If  $f = 40$  MHz, then  $T_{eff} \approx 10^{-3}$  K. Thus the lowest effective noise temperature attainable with an isolated Josephson junction oscillating at 40 MHz is of the order of one millikelvin. However, in the circuit proposed for thermometry, the shunt resistor would damp the noise emf generated by the junction. The effective noise temperature of the combination would be given by an expression of the same form as equation (7), with a suitably defined effective resistance for the junction. Inspection of equation (7) shows that it would be possible to measure temperatures below  $T_{eff}$  with a very small shunt resistance.

In addition to the two tunneling processes we have discussed, real junctions can transmit some current by ohmic leakage through the barrier. This would presumably generate Johnson noise. It can be considered as part of the shunt conductance with no further complication of the problem.

Thus the fundamental limitations to noise thermometry with the Josephson effect that we are aware of would permit its use in the temperature range from about  $10^{-3}$  K up to the critical temperatures of conveniently available superconductors, near 10 K. However, a real system is subject to noise from sources other than those considered by Stephen. There are external sources such as radio stations, atmospheric and galactic noise, etc, which can be eliminated with a screened enclosure. There are also strange noise-generating processes within the junction which can only be eliminated by patient development.

So far we have discussed fundamental limitations which are common to measurements by both spectrum analysis and frequency counting. We will now discuss some points which are peculiar to frequency counting.

First, random error. A simple analysis shows that the rms scatter  $\Delta T$  on the value  $T$  of a noise temperature measured by the frequency counting method is

$$\Delta T = T \sqrt{2/n} \quad (8)$$

where  $n$  is the number of measurements of frequency used to compute the variance of the fluctuations. This is a purely random error arising from the statistics of measuring a fluctuating quantity.

A frequency counter also introduces a systematic error, which arises because it only counts complete cycles. Thus the measured frequency is always an integral multiple of  $\tau^{-1}$ , where  $\tau$  is the gate time.

If a counter is set to measure a signal with an arbitrary frequency  $f$ , then its reading will switch randomly between the two integral multiples of  $\tau^{-1}$  bracketing  $f$ . Let us denote these quantities  $f_0$  and  $(f_0 + \tau^{-1})$ . Assuming that there is no phase correlation between the signal and the time base of the counter, then a fraction  $1 - (f - f_0) \tau$  of the readings will be  $f_0$  and a fraction  $(f - f_0) \tau$  will be  $(f_0 + \tau^{-1})$ . Thus the mean value of a large number of readings is just equal to  $f$ . However, this also introduces an extra fluctuation in the measured frequency. The variance  $\sigma_f^2$  of this extra fluctuation is

$$\sigma_f^2 = (f - f_0) \tau^{-1} - (f - f_0)^2. \quad (10)$$

In practice,  $f$  will fluctuate also, so we should average  $\sigma_f^2$  over all values of  $(f - f_0)$  between zero and  $\tau^{-1}$ . Doing this, we find the mean variance  $\sigma_c^2$  of the extra fluctuations introduced by the counter is

$$\sigma_c^2 = (6\tau^2)^{-1}. \quad (11)$$

The variance of the total observed fluctuations will then be the sum of  $\sigma_c^2$  (equation 5) and  $\sigma_c^2$  (equation 11). The effect is to introduce a shift  $\delta T$  in the measured temperature, where

$$\delta T = T (\sigma_c^2 / \sigma^2)$$

or

$$\delta T = \varphi_0^2 / (12 kR\tau). \quad (12)$$

It is a trivial matter to correct measured temperatures for this effect, but the extra fluctuation increases the random scatter of the measurements and will ultimately limit the resolution of temperature when  $\delta T$  exceeds  $T$ . Thus the minimum resolvable temperature  $T_{\min}$ , taking  $n$  readings with a counter of gate time  $\tau$ , is

$$T_{\min} = \delta T \sqrt{2/n}$$

or

$$T_{\min} = \frac{\varphi_0^2 \sqrt{2/n}}{12 kR\tau} \quad (13)$$

or

$$T_{\min} = 3.5 \times 10^{-8} (R\tau\sqrt{n})^{-1}.$$

Thus a fairly long gate time is desirable for measuring very low temperatures. With  $R = 10^{-5}\Omega$  and  $\tau = 1$  second, millikelvin resolution could be obtained in a run of a few minutes.

The conclusion, then, is that none of the fundamental theoretical limitations on this type of thermometry, which we have been able to find, would preclude its convenient use at temperatures down to one millikelvin, or its use at even lower temperatures with some extra precautions.

### 3.3 Experimental Tests

The linewidth of Josephson oscillation at frequencies of 30 MHz and below has been measured by A. H. Silver and J. E. Zimmerman, of the Ford Scientific Laboratory, and published jointly with one of us. [17] They found that equation (4) described the observed relationship between linewidth and  $R$  and  $T$ , to within the experimental error (about 5%), in the range  $1.7 \times 10^{-10}\Omega < R < 2.6 \times 10^{-5}\Omega$ ;  $1.4\text{K} < T < 8\text{K}$ . At the time of making these measurements, these authors did not know the exact numerical coefficient of equation (4). This result demonstrates the feasibility of thermometry in the temperature range above 1.4 K as well as the feasibility of observing the narrower linewidths required for thermometry at lower temperatures.

We have constructed a prototype thermometer based on frequency counting. The layout is shown in figure 6. The signal from the oscillating Josephson junction is coupled by a tuned transformer and coaxial line into a communications receiver. In the receiver the signal is amplified and mixed with another signal from a tunable local oscillator (L.O.) to generate a signal at an intermediate frequency near 455 kHz. This intermediate frequency is measured directly with a frequency counter and recorded on paper tape. We have a simple computer program to compute the variance of the fluctuations in the frequencies recorded on the tape and hence the noise temperature. This program corrects the data for the extra fluctuations introduced by the counter, which we discussed in section 3.2.

In analyzing white noise, care must be exercised to discriminate against other sources of noise, such as flicker noise, which have an anomalously large part of their spectral distribution at very low frequencies (the power spectrum for flicker noise is proportional to  $f^{-1}$ ). These will always interfere with measurements requiring long periods of time. Methods of analyzing and handling flicker noise have been developed by Barnes<sup>[18]</sup> and Allen.<sup>[19]</sup> Following them, and the suggestions of Dr. D. Halford of this laboratory, we have arranged our computer program to calculate the variance  $\sigma^2$  from the formula

$$\sigma^2 = \frac{1}{2} \overline{(f_i - f_j)^2} \quad (14)$$

where  $f_i$  and  $f_j$  are two successive measured frequencies. The advantage of equation (14) over equation (5) is that (14) is only sensitive to fluctuations with period comparable to the interval between successive measurements or less, whereas (5) is sensitive to fluctuations with period up to the total length of time required to take all the data. It is also

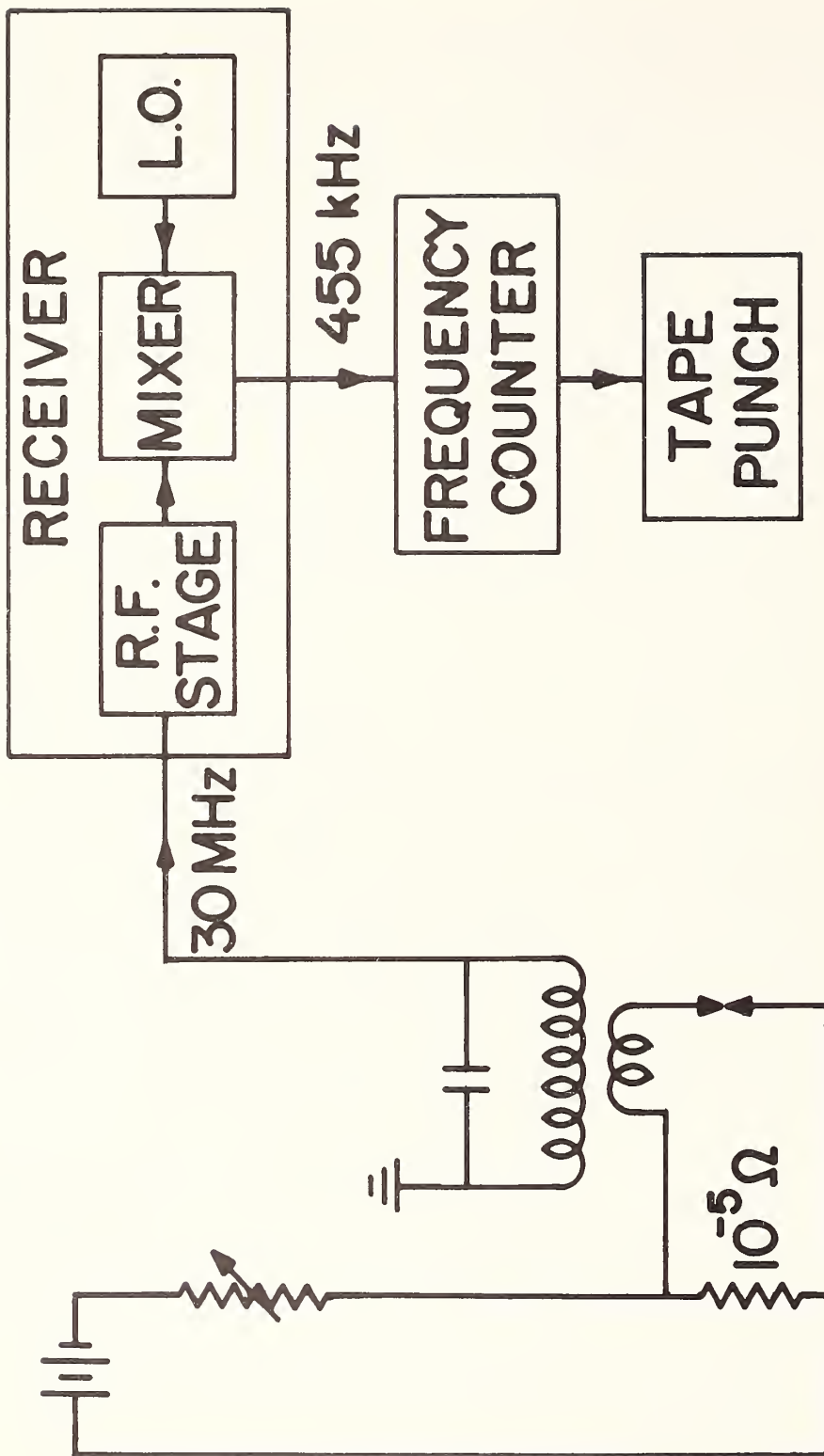


Figure 6. Arrangement for noise thermometry by frequency counting.

helpful to use as short a gate time  $\tau$  as possible, since this increases the sensitivity of the variance  $\sigma^2$  to white noise. The dependence of  $\sigma^2$  on  $\tau$  for noise sources with other commonly found power spectra is weaker. As a check on the frequency spectrum of the observed fluctuations, our computer program also calculates  $\sigma^2$  from equation (14) taking measurements with double and quadruple intervals. That is, as well as taking  $j = i + 1$ , it takes  $j = i + 2$  and  $j = i + 4$ . If we are observing pure white noise, this leaves the value of  $\sigma^2$  unchanged apart from random scatter. If there is a component with a different power spectrum, then these three values of  $\sigma^2$  will differ significantly.

The layout we use for the oscillating junction and shunt resistor is shown in figure 7. It incorporates some suggestions made to us by Dr. J. E. Zimmerman of the Ford Scientific Laboratory. The junction is formed between the etched tip of the Nb-Zr wire and the niobium block when the whole structure is compressed by the 0-80 screw. The brass block functions as the shunt resistor. The layer of lead-tin solder is "tinned" onto its surface and pressed against the niobium block when the assembly is bolted together, forming a superconducting joint of high critical current. The coupling hole forms the single turn primary of the output transformer. The secondary is a 15-turn coil wound inside the coupling hole and tuned to 30 MHz with a 500 pF capacitor. The dominating RF impedance in the primary circuit is the junction itself.

This system functions at 4K. By patient manipulation of the adjusting screw it is possible to obtain stable Josephson oscillation and record a realistic noise temperature. However, the junction does have a strong tendency to generate multiple quantum transitions which mix with signals from the receiver to generate a complex spectrum of spurious resonances which are noisier than the desired oscillation.

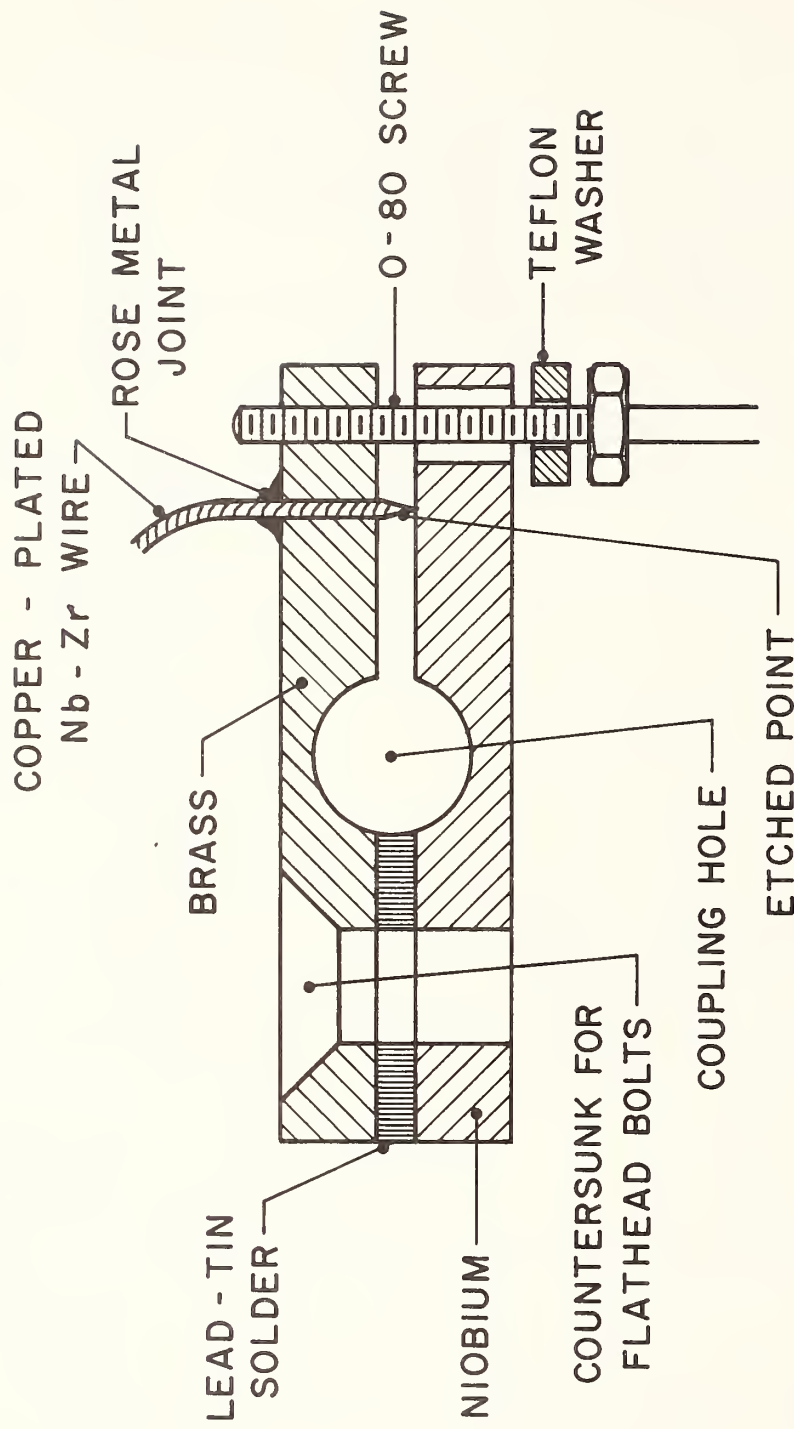


Figure 7. Details of junction, bias resistor, and primary of output transformer. The gap between the niobium and brass blocks is exaggerated for clarity.

We are experimenting with buffer amplifiers to try to cure this problem. We have mounted the junction in an experimental  $\text{He}^3$  -  $\text{He}^4$  dilution refrigerator built by Dr. R. Radebaugh and Dr. J. D. Siegwarth of this laboratory. This refrigerator is capable of providing a continuous operating temperature of 0.02 K for tests of thermometry. Some minor troubles remain to be eliminated before we test noise thermometry with the Josephson effect at this temperature.

#### 4. Possible Contribution of Superconducting Devices to Nuclear Magnetic Resonance Detection

Nuclear Magnetic Resonance (NMR) is the resonant interaction of a radio-frequency field with the Larmor precession of the magnetic moments of atomic nuclei in a steady magnetic field. Its intensity, spectral distribution, and transient response give information about the multipole moments of nuclei, their isotopic abundance, and their interaction with their immediate surroundings. Interesting information about the solid and liquid states can be inferred from this. Our purpose here is to consider possible ways to improve the sensitivity of detection of this phenomenon by the application of superconductivity.

After a brief sketch of the essential features of NMR as they affect detection schemes, we will discuss the relative merits of piecemeal improvements to the systems in current use and the possibility of using a flux quantum magnetometer. We will express all quantities in S. I. units.

It is convenient to represent the combined magnetic behavior of all the nuclei in a specimen in terms of the complex magnetic susceptibility  $\chi$  introduced by Bloch.<sup>[20]</sup> This is a tensor whose components are functions of frequency. At zero frequency it is usually more or less isotropic and is just the contribution  $\chi_0$  of the nuclei to the static magnetic susceptibility of the specimen. If the nuclei are temporarily disturbed,

this longitudinal magnetization relaxes back to equilibrium in a characteristic time  $\tau_1$ . The other important components of  $\chi$  occur in the plane transverse to the steady magnetic field at frequencies near the resonant frequency  $\omega_0$ . There is a component  $\chi'$  in phase with an applied RF field and a component  $\chi''$  in quadrature. The transverse magnetization relaxes to the steady state with a characteristic time  $\tau_2$ . If  $\chi_0''$  is the peak value of  $\chi''$ , observed with a small RF field exactly on resonance, then

$$\chi_0 = 2\chi_0''/\omega_0\tau_2. \quad (15)$$

In a complicated system with several resonances, each contributes an amount given by equation (15) to  $\chi_0$ .

In present-day schemes for detecting NMR, the specimen is placed in the tank coil of a resonant LC circuit. The resonant frequency of the circuit is then perturbed by  $\chi'$ , while  $\chi''$  contributes to the absorption of power and hence influences the Q factor when the Larmor frequency is brought into coincidence with the resonant frequency of the circuit. Both these effects may be detected with an RF bridge with a sensitive receiver.<sup>[21]</sup> The sensitivity of a bridge to small changes in  $\chi'$  and  $\chi''$  increases as the RF level is increased, but a limit is set by the degrading of all components of susceptibility at high levels due to saturation of the resonance. At the optimum RF level  $\chi_0$ ,  $\chi'$ , and  $\chi''$  are all reduced to half their equilibrium values. The minimum detectable equilibrium value of  $\chi''$  under this condition is then<sup>[22]</sup>

$$\chi'' = \left[ \frac{32 F k T_0 \Delta \gamma^2 \tau_1 \tau_2}{\mu_0 \eta U \omega_0 Q} \right]^{\frac{1}{2}} \quad (16)$$

where  $F$  is the noise figure and  $\Delta$  the bandwidth of the receiver,  $T_0$  is the ambient temperature,  $U$  and  $\eta$  are the volume and the filling factor of the tank coil, and  $\omega_0 = \gamma H_0$ , where  $H_0$  is the steady field causing Larmor precession at frequency  $\omega_0$ . Achievement of this theoretical sensitivity in practice requires great stability of the oscillator and bridge components

in order to avoid microphonic noise. This makes it necessary to search for resonances by varying the magnetic field while keeping the frequency constant. This problem can be avoided by making the tuned circuit part of an oscillator operating at a low level.<sup>[23, 24]</sup> Variations in Q then cause variations in the level of oscillation which can be observed with a receiver. The ultimate sensitivity of this arrangement is given by an expression similar to equation (16). In practice it is difficult to achieve a good overall noise figure F over a wide range of RF levels because of the need to operate the active components in non-linear parts of their characteristics.<sup>[25]</sup> However, an optimum noise figure of 2 has been reported in the literature.<sup>[23]</sup> Equation (16) represents the performance with which any improved detection system must compete.

#### 4.1 Piecemeal Improvements

Looking at the formula in equation (16) for the sensitivity of the NMR detectors currently in use, it is obvious that some improvements can be made simply by replacing various components with superconducting versions.

Turning first to the factor  $FkT_0$  in equation (16), there is scope for a superconducting preamplifier, such as a parametric up-converter or a linear cryotron amplifier,<sup>[26]</sup> to gain an order of magnitude by operating at a low effective temperature. This has been achieved by Silver and Zimmerman<sup>[27]</sup> using the Josephson effect. Their device suffers from the limitation that it only operates with a very low RF level, so that its performance would fall short of the optimum expressed by equation (16) except when the relaxation times  $\tau_1$  and  $\tau_2$  are long. The advantage of low temperature operation has also been obtained with field effect transistors by Miyoshi and Cotts,<sup>[28]</sup> and by Alderman.<sup>[29]</sup>

The limitation is that the effective value of  $T_0$  is controlled by all the lossy components in the input circuit, including the tank circuit and

specimen. Thus if the specimen accounts for a significant part of the damping of the tank circuit it too must be cooled. In general, this has the effect of increasing the components of susceptibility, but also increases the relaxation time  $\tau_1$ . It may not always be desirable to work with a cold specimen, and if not the attainable effective noise temperature is limited.

Another obvious application of superconductivity is in raising the  $Q$  of the tank circuit. This has been investigated by Persyn, Victor, and Rollwitz,<sup>[30]</sup> who operated a system at 0.95 MHz with a superconducting tank circuit. Because of their choice of superconductor and layout (lead coated copper wires), they were restricted to work at flux densities less than 20 millitesla. They observed a considerable improvement in sensitivity over a non-superconducting system working at the same low field. However, the factor  $\omega_0$  in equation (16) requires us to consider flux densities approaching 1 tesla. Further development is required on high- $Q$  circuits at these high fields. Once again, the limit to attainable performance may be set by loss in the specimen.

The presence of superconducting material will cause a distortion of the magnetic field at the specimen, and it is important to preserve the homogeneity of the field to avoid broadening the resonance. In order to operate in a high field, the tank coil would be made of a type II superconductor, whose magnetic effect in a transverse field can be represented by a large diamagnetic susceptibility. Field distortion would be caused by unsuitable geometry of the coil or by variations in its effective magnetic susceptibility due to uneven flux pinning. The simplest geometry to use would be a thin film of superconductor deposited on an insulating cylinder with a narrow helical scratch to form it into an inductive coil. If we approximate this geometry by an infinitely long cylinder of radius  $r$  coated with a film of susceptibility  $\chi$  and thickness  $d$ , then a uniform

transverse field  $H_0$  outside the cylinder would generate a uniform field  $H$  inside, where

$$H = H_0 (1 + \chi d/r)^{-1}. \quad (17)$$

In this expression,  $\chi$  cannot exceed  $H^2/H_c^2$ , where  $H_c$  is the thermodynamic critical field of the superconductor. Variations in  $\chi$  must be less than  $\chi$  itself. It would be perfectly feasible to use a film 1000 Å thick, with  $r$  of the order of 1 cm. Field distortion should therefore be below the part per million level.

#### 4.2 Magnetometry

There are reported in the literature several very sensitive superconducting magnetometers.<sup>[31]</sup> Some of these operate by modulation of the inductance of a circuit carrying a persistent current, thereby generating an alternating voltage proportional to the magnetic flux,<sup>[32, 33]</sup> while others are essentially flux-quantum counters which depend on the properties of multiple Josephson junctions<sup>[34, 35]</sup> and can be sensitive to changes in magnetic flux of  $10^{-8}$  quanta. Recently Mercereau<sup>[36]</sup> reported a reliable, engineered version of a magnetometer based on flux quantization capable of detecting changes in flux density of  $10^{-14}$  tesla.

The scheme of NMR detection we propose to analyze is one in which the change in flux density  $\delta B$ , resulting from the change in static nuclear susceptibility  $\chi_0$  induced by NMR, is detected with a superconducting magnetometer. This was first suggested by Pierce.<sup>[33]</sup> The crucial practical problem in this scheme would be supplying the RF field to induce NMR without interfering with the very sensitive magnetometer. This might be accomplished simply by avoiding the modulation frequency in the inductance modulated magnetometers if the readout system were sufficiently linear to avoid excessive mixing. Other possible schemes would supply RF power in pulses,<sup>[33]</sup> or as ultrasonic phonons when the nuclei under study possess quadrupole moments. Another problem is that the

steady magnetic field must be stable to  $10^{-14}$  tesla. This can only be accomplished with superconductors, and it precludes sweeping or modulating the magnetic field. These problems are not trivial, and the purpose of this analysis is to discover if they are worth attacking.

In order to compare this system with detection by power absorption, let us assume that sufficient RF field is applied to saturate the resonance to the extent of halving  $\chi_0$  from its equilibrium value. This corresponds to the optimum RF level for detecting  $\chi'$  and  $\chi''$ . The change in magnetic flux density  $\delta B$  corresponding to the minimum detectable NMR signal given by equation (16) is then

$$\delta B = \frac{1}{2} \mu_0 \chi_0 H_0 = \left[ \frac{32 F k T_0 \Delta \mu_0 \tau_1}{\eta U \omega_0 Q \tau_2} \right]^{\frac{1}{2}}. \quad (18)$$

A superconducting magnetometer can only compete in sensitivity with the present-day RF spectrometers mentioned in our introduction if the quantity  $\delta B$  given by equation (18) exceeds  $10^{-14}$  tesla. For a numerical comparison, let us take  $U = 1 \text{ cm}^3$ ,  $\eta = 1$ ,  $Q = 100$ ,  $\Delta = 1 \text{ Hz}$ ,  $\omega_0 = 10 \text{ MHz}$ . This flattens RF spectrometers at ambient temperature by a factor greater than unity but less than 10. Substituting these numbers into equation (18) we find

$$\delta B \approx 5 \times 10^{-15} \sqrt{\tau_1 / \tau_2}. \quad (19)$$

Thus if  $\tau_1 = \tau_2$ , as often happens in liquids for example, the best sensitivity obtainable with a superconducting magnetometer is approximately equal to that of a good RF bridge or marginal oscillator operating at ambient temperature. Clearly there would be no reward for the considerable effort of development. However, if  $\tau_1 \gg \tau_2$  the superconducting magnetometer would begin to show some advantage. This condition is often observed in solids, particularly at low temperatures.

There are other unusual circumstances when the superconducting magnetometer would be advantageous: for example, Pierce's magnetometer<sup>[33]</sup> was designed for a non-destructive readout of the orientation of the spins of a polarized sample of <sup>3</sup>He in a nuclear gyro. There was no problem with sensitivity because of the metastable polarization of the spins.

#### 4.3 Conclusions

It appears that using a cold input circuit (possibly including a superconducting preamplifier) and a superconducting high-Q tank circuit can each raise the sensitivity of an otherwise conventional NMR detector by an order of magnitude if the specimen permits. The impressive sensitivity of superconducting magnetometers gives an advantage to NMR detection only in unusual circumstances, such as very long  $\tau_1$ .

This last statement appears surprising unless one understands how large the flux quantum is compared with other fundamental quantities. In order to change the magnetic flux linking a cylinder 1 cm long, of arbitrary cross section area, by one flux quantum it would be necessary to flip approximately  $10^{16}$  nuclear spins within its volume. One's respect for NMR as a sensitive probe of matter is enhanced by this reflection.

## 5. Overall Conclusions

In this report we have given a recipe for fabricating permanent niobium-lead Josephson junctions and a design for a millikelvin noise thermometer which is presently in the prototype testing stage. Both of these appear to be real contributions to the practical application of the Josephson effect. An examination of the possibility of applying superconductivity to NMR detection revealed a less promising situation.

## APPENDIX

### A Review of the Josephson Effect

Prepared for the IEEE Transactions on Instrumentation  
and Measurement

The original discovery of the Josephson effect followed the classic pattern which is optimistically described in many textbooks of elementary science but quite rarely encountered in real life. It is a very striking manifestation of quantum mechanics on an unusually large scale, which was originally predicted theoretically by B. D. Josephson<sup>[37-39]</sup> in 1962. He published his theory under the cautious title "Possible New Effects in Superconductive Tunneling," and it was quickly challenged by several other eminent theorists. There was a vigorous debate until the first experimental observation of the effect by Anderson and Rowell<sup>[40]</sup> the following year. In view of the controversy they, too, used cautious words and reported the "Probable Observation of the Josephson Superconducting Tunnel Effect." With the accumulation of more experimental evidence the doubts evaporated, and published statements became bolder. Since then there has been an exciting period of invention of devices, based on the Josephson effect, which promise to revolutionize many aspects of electronics. The purpose of this article is to sketch the main features of the effect itself and to describe some of these applications.

The Josephson effect occurs at a Josephson junction, which is a weak electrical contact between two pieces of superconducting metal. We will discuss Josephson junctions and their highly non-linear electrical characteristics in the following section. Thereafter we will describe briefly some devices, based on these characteristics, which range in state of development from early concepts to well engineered instruments. In general, these devices are well adapted to handling very small signals

with a very low noise level. Many of them have a very wide dynamic range. Often their calibration can be related directly to fundamental constants, making absolute measurements possible. Since the Josephson effect requires superconductivity, all these devices must operate at a very low temperature, usually provided by a bath of liquid helium.

### Josephson Junctions

There are several practical ways to make the weak electrical contacts required by the Josephson effect. An ideal junction might consist of two superconductors separated by a vacuum gap about  $10\text{ \AA}$  ( $10^{-7}\text{ cm}$ ) wide and perhaps a square millimeter in area. Electrons would cross this gap by the quantum mechanical tunnel effect. <sup>[39, 41]</sup> The nearest practical approach consists of a strip of thin film of one superconductor deposited on an insulating substrate such as glass, quartz, or sapphire. Its surface is covered with an insulating barrier of the desired thickness (usually by oxidation of the metal), and then a strip of thin film of the second superconductor is deposited across the first to complete the junction. The barrier does not need to be an insulator. A layer of normal metal such as copper, about  $10,000\text{ \AA}$  thick, will work instead. <sup>[42]</sup> Another approach is to use a continuous strip of superconducting thin film with a very narrow constriction <sup>[43]</sup> (a few micrometers wide). The electrical characteristics of this microbridge structure differ from those of crossed film junctions, but the similarities are sufficient for many practical purposes. An intermediate approach is to press a slender point on one superconductor lightly against the other to form a point contact junction. <sup>[6]</sup> It is not quite clear whether a surface layer formed by atmospheric corrosion forms an insulating barrier, or if the narrow contact area functions as a microbridge. However, point contacts have the great advantage that they can be adjusted while in operation and they work very well. The more permanent structures such as crossed film junctions and microbridges have the compensating advantage of greater mechanical stability.

Superconductors commonly used to make Josephson junctions are lead, tin, indium, niobium, tantalum, etc. It is not important whether the same or two different superconductors are used to form a junction.

The electrical characteristics of these junctions depend on how they are made,<sup>[44, 45]</sup> but one feature they all have in common is the ability to pass a limited current (in the range from a few  $\mu\text{A}$  to a few mA) without any voltage appearing. A somewhat idealized I-V curve for a crossed film junction is shown in figure 8. If the current passing through the junction exceeds  $I_c$  (fig. 8) a voltage appears and there is often an unstable region of negative dynamic resistance. There is a characteristic voltage of the order of a millivolt, determined by the energy gaps of the superconductors, at which the current rises sharply before settling down to an ohmic response at high voltage. Microbridges differ from crossed film junctions mainly by the absence of the low current region at intermediate voltage.

The magnitude of  $I_c$  is very sensitive to a magnetic field applied in the plane of the junction. Figure 9 shows a plot of  $I_c$  versus magnetic flux density for an ideal crossed film junction. Similar curves have been observed in the laboratory.<sup>[46]</sup> The vertical scale depends critically on the thickness of the insulating barrier, while the horizontal scale is controlled by the width of the junction and the properties (penetration depths) of the superconductors. The periodicity is caused by quantum interference between electrons crossing different parts of the barrier. It is analogous to optical diffraction at a narrow slit. The analogue of optical interference between two slits can be created by connecting two Josephson junctions in parallel in a superconducting circuit as shown in figure 10. The curve shown in figure 9 then becomes the envelope of an interference pattern of much shorter period. This period corresponds to the quantum of magnetic flux  $h/2e \approx 2 \times 10^{-15}$  Weber. ( $h$  is Planck's constant and  $e$  is

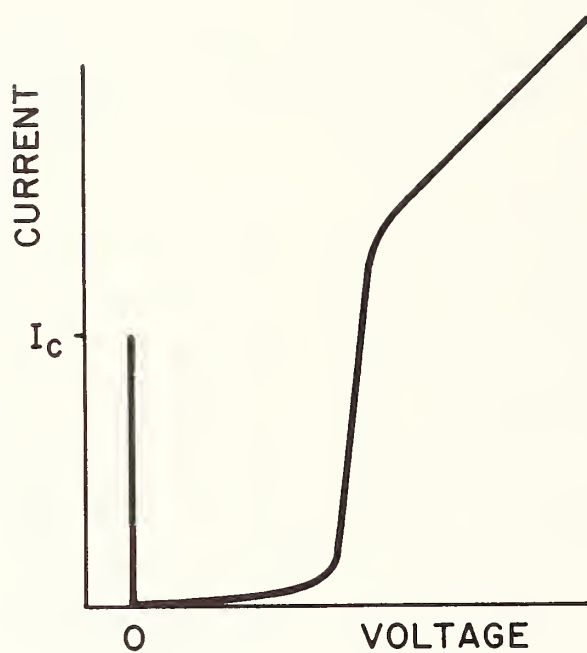


Figure 8. Current versus voltage characteristic of a thin film Josephson junction.

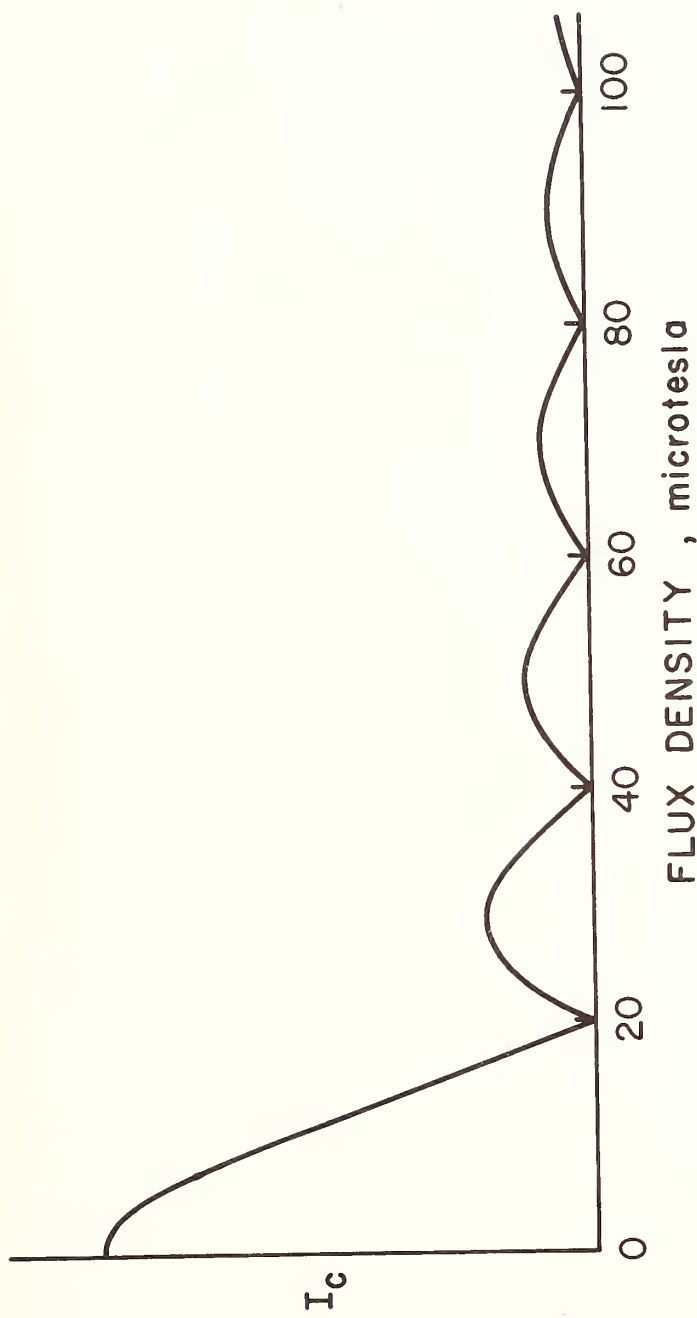


Figure 9. Dependence of  $I_c$  (fig. 8) on applied magnetic field. The scales depend upon the geometry of the junction.

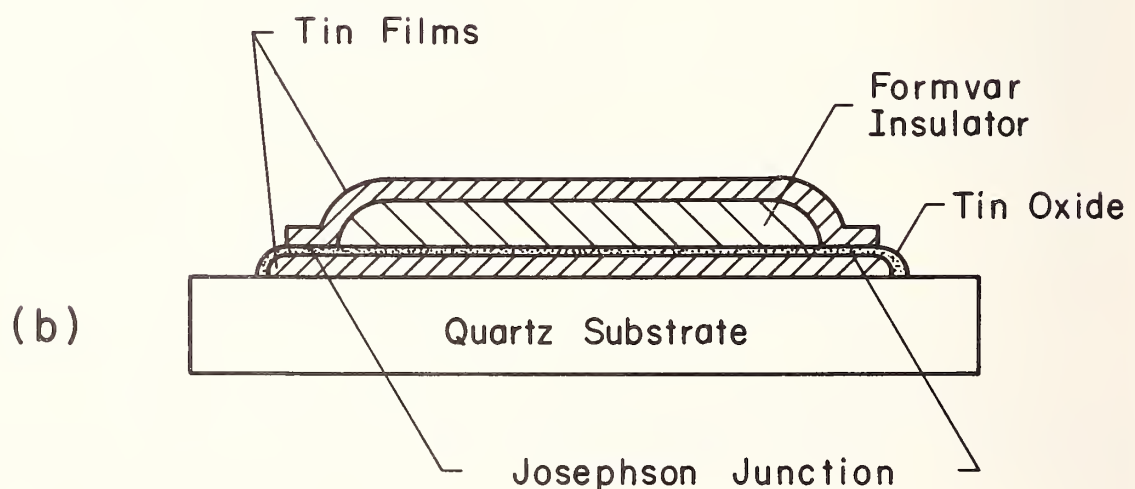
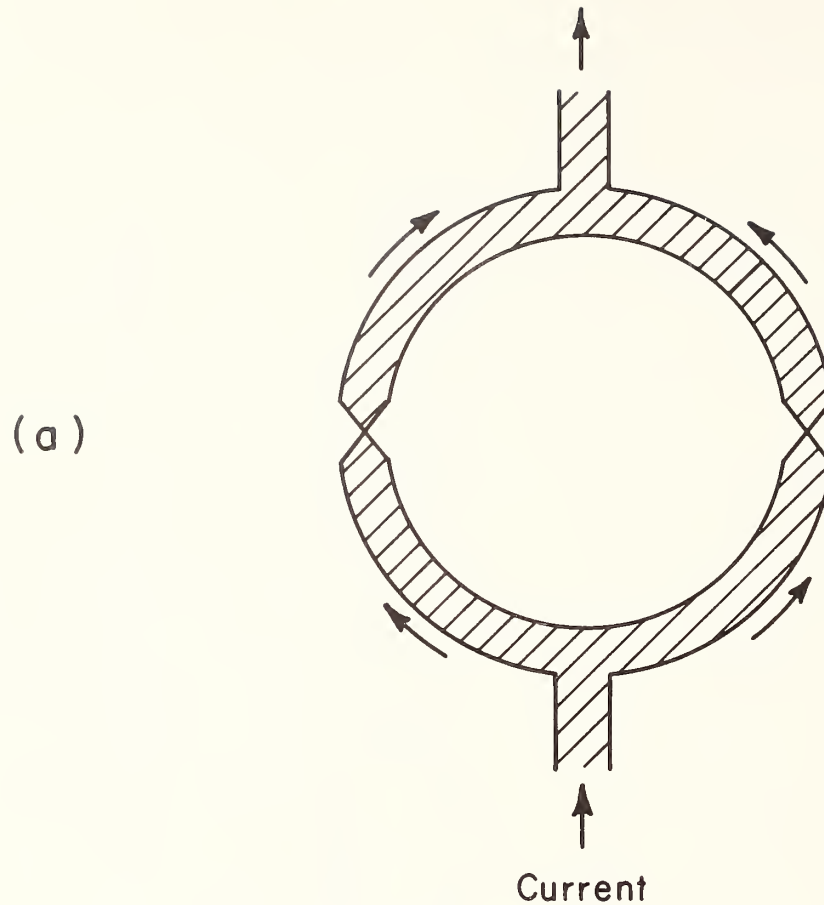


Figure 10. The quantum interferometer, a) ideal, b) early practical version (ref. 47).

the electron charge.) Each minimum in the interference pattern occurs when a whole number of magnetic flux quanta link the superconducting loop. This arrangement has become known as a quantum interferometer.<sup>[47]</sup> It has obvious applications to magnetometry and other arts.

If a resonant circuit is connected to a Josephson junction a peak appears<sup>[48]</sup> in the direct current vs. voltage characteristic as shown in figure 11. The voltage  $V$  at which the peak appears is related to the resonant frequency  $f$  of the circuit by  $hf = 2eV$ . This corresponds to approximately 484 MHz per  $\mu$ V.

If a radio frequency or microwave signal is addressed to the junction, the direct current vs. voltage relationship becomes profoundly modified as shown in figure 12. It develops a series of steps at equal intervals of voltage.<sup>[49]</sup> Once again the voltage interval  $V$  is related to the frequency by  $hf = 2eV$ .

Finally, if a receiver is connected to the junction, a coherent oscillation<sup>[49, 50]</sup> can be detected at the same frequency  $f = 2eV/h$ . The waveform is usually non-sinusoidal, so harmonics of this frequency can also be detected at sub-multiples of the fundamental voltage. These are illustrated by an actual recorder chart shown in figure 13. The receiver was tuned to 43 MHz and the odd signal shape was a result of lock-in detection. This oscillation is a quantum mechanical effect. A pair of electrons with charge  $2e$  falls through a potential drop  $V$ , and the energy  $2eV$  which they gain is radiated away as a quantum  $hf$ . Frequencies ranging from a fraction of 1 Hz<sup>[51]</sup> to 10 GHz<sup>[52]</sup> have been observed.

### Applications of the Josephson Effect

With some exercise of ingenuity it is possible to devise sensors of almost anything known to man using the Josephson effect, and most of them would probably perform rather well. We will restrict our discussion to devices which at least exist in prototype form.

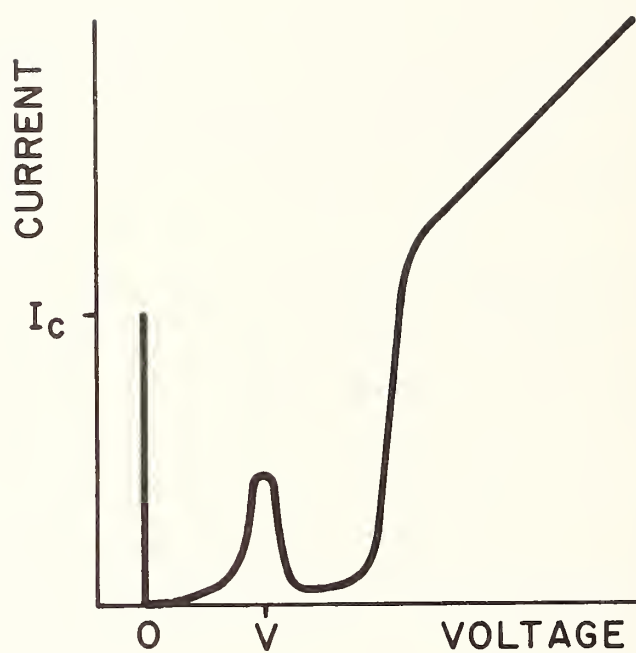


Figure 11. Current versus voltage characteristic of a thin film Josephson junction connected to a circuit with a resonance at frequency  $f = 2eV/h$ .

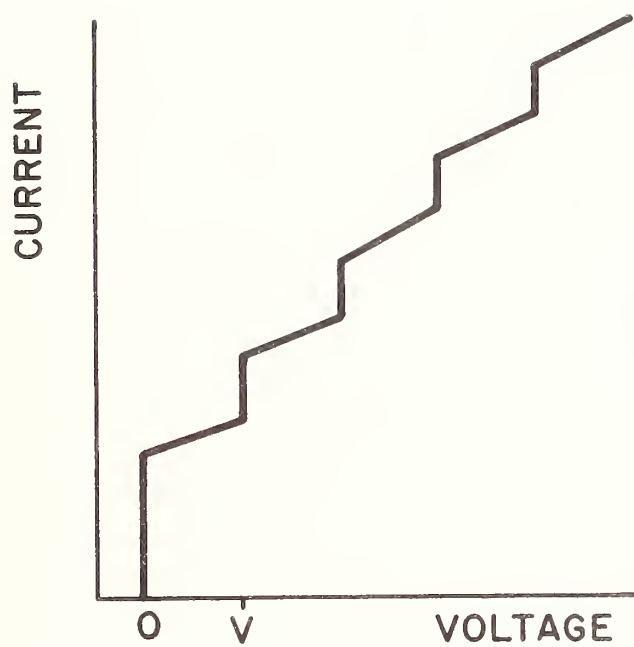


Figure 12. Current versus voltage characteristic of a Josephson junction irradiated at a frequency  $f = 2\text{eV}/\text{h}$ .

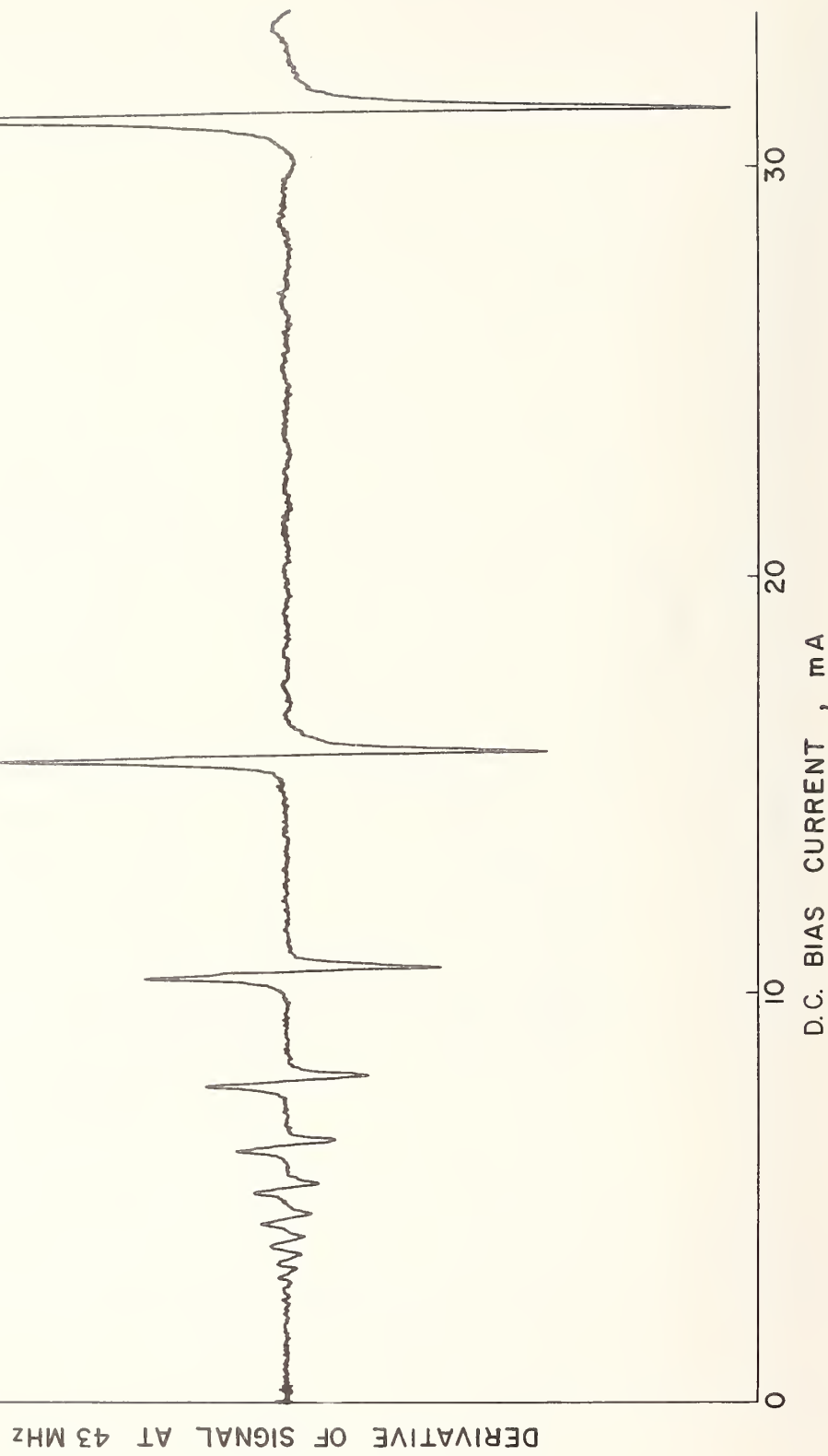


Figure 13. Josephson oscillation. The response of a receiver tuned to 43 MHz is displayed as a function of DC bias on the Josephson junction.

Perhaps the most obvious application of the Josephson effect is to magnetometry. The quantum interferometer (fig. 10) is clearly a very sensitive sensor of magnetic field. The most advanced magnetometer to date was described recently by Mercereau.<sup>[36]</sup> It is based on a variation of the quantum interferometer using a superconducting ring with only one microbridge. By coupling this structure inductively to a resonant L-C circuit it is possible to measure its impedance at 30 MHz. This turns out to be a periodic function of both steady and RF magnetic fields, the period corresponding to the flux quantum. Mercereau described a well engineered instrument capable of detecting changes in steady magnetic flux of  $10^{-3}$  quanta. Because of the macroscopic nature of the quantization in the superconducting state the philosophical problems this appears to raise can be resolved.

A sensor of magnetic field can also sense electric current, and Clarke<sup>[53]</sup> has made this the basis for a very sensitive null detector, illustrated in figure 14. The device consists of a short length of superconducting niobium wire with a blob of superconducting lead-tin solder frozen onto it. The solder does not wet the niobium because of the presence of an oxide layer. Once in many attempts a pair of Josephson junctions are formed, probably at the ends of the solder blob. They then form a quantum interferometer which is sensitive to the circumferential magnetic field due to the current in the niobium wire. Clarke reports that this device can detect  $10^{-6}$  A. Because of the very small inductance of the niobium wire, this current would build up in one second if driven by a voltage of  $10^{-15}$  V. The device is therefore a very sensitive detector of a voltage null in a low impedance circuit. By connecting the ends of the niobium wire together, this device can be made into a magnetometer. A change in magnetic flux linking the loop would be opposed by a persistent induced current, which would be sensed by the quantum interferometer. The minimum detectable change in magnetic flux density is once again  $10^{-14}$  tesla.<sup>[35]</sup>

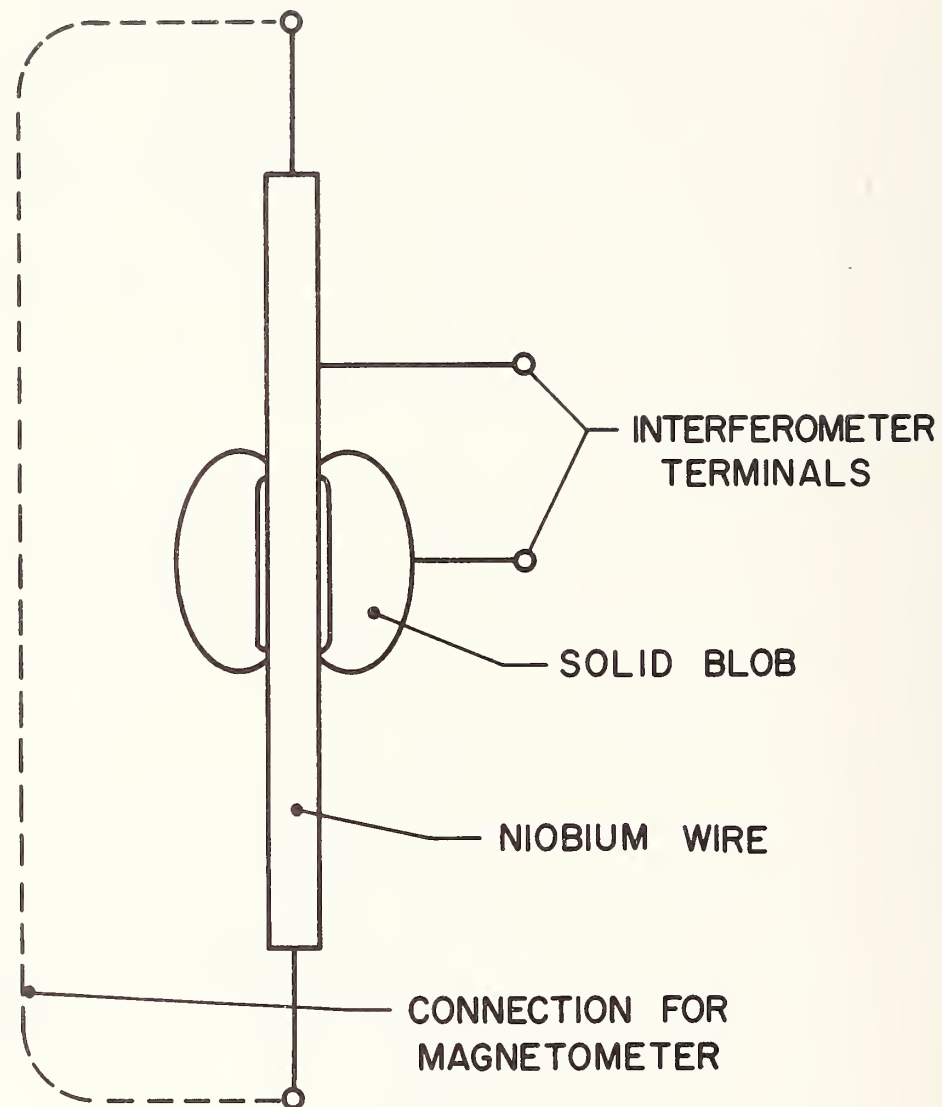


Figure 14. The Clarke null detector.

Both the magnetometers we have mentioned are only sensitive to changes in magnetic field. They require special precautions to set the zero for absolute measurements.

Meservey<sup>[54]</sup> has suggested that by careful attention to geometry it would be possible to construct a sort of absolute ammeter, using a quantum interferometer to relate the ampere to the flux quantum.

Another application of the sensitivity of the Josephson effect to magnetic field is Matisoo's tunneling cryotron.<sup>[55]</sup> In this device the gate strip of a thin film cryotron<sup>[56, 57]</sup> is replaced by a thin film Josephson junction. An insulated control strip is laid across the junction (fig. 15). When a current is passed through the control strip it generates a magnetic field which affects the maximum supercurrent  $I_c$  which the junction can pass as shown in figure 9. The I-V characteristic of the gate is illustrated in figure 16. If it is biased to the operating point A (fig. 16), a small pulse of current in the control strip can depress  $I_c$  below the operating current and cause the device to switch to the operating point B at a voltage of the order of a millivolt.

This device was designed for a computer element. Its advantage over the original thin film cryotron is its high resistance in the switched state, which permits very fast switching. A switching time of  $10^{-10}$  seconds has been achieved for diverting current from one branch of a network to another.

Turning now to the Josephson oscillation, it too can be used to measure very low voltage. The record is held by Silver and Zimmerman,<sup>[51]</sup> who indirectly observed the oscillation of a Josephson junction at 0.2 Hz, corresponding to a DC bias voltage of  $4 \times 10^{-16}$  volts. They used the junction both as oscillator and mixer, to mix the very feeble signal from the self-oscillation with a much stronger one at 30 MHz. The resulting amplification by parametric up-conversion was sufficient to make it observable.

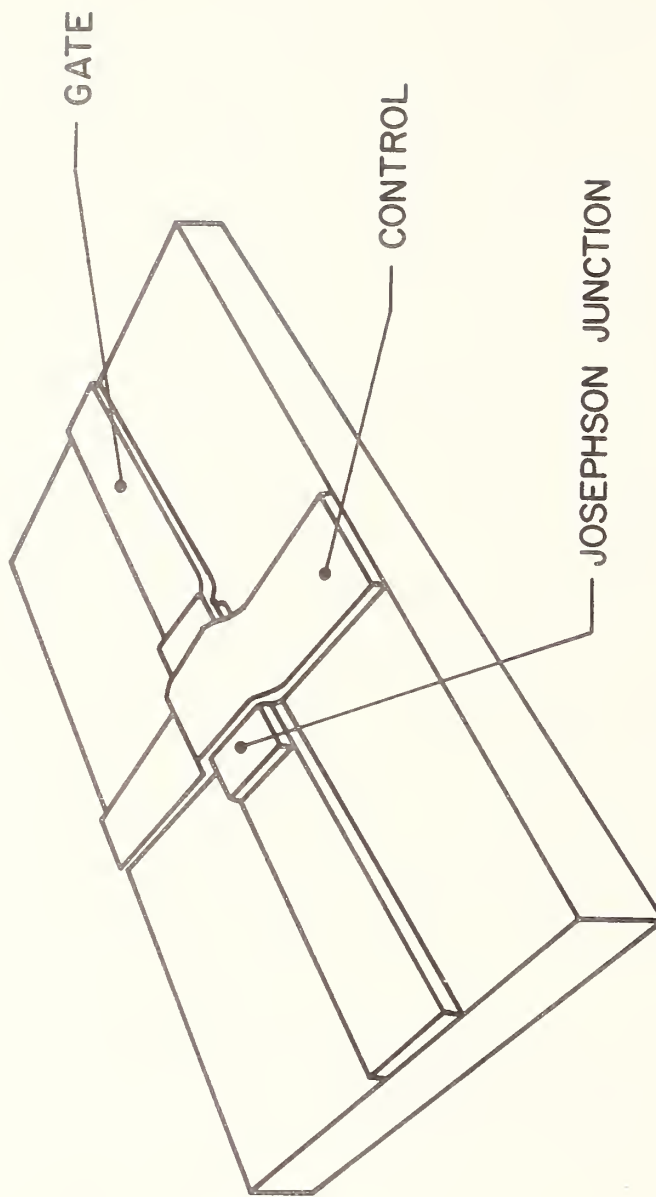


Figure 15. The tunneling cryotron.

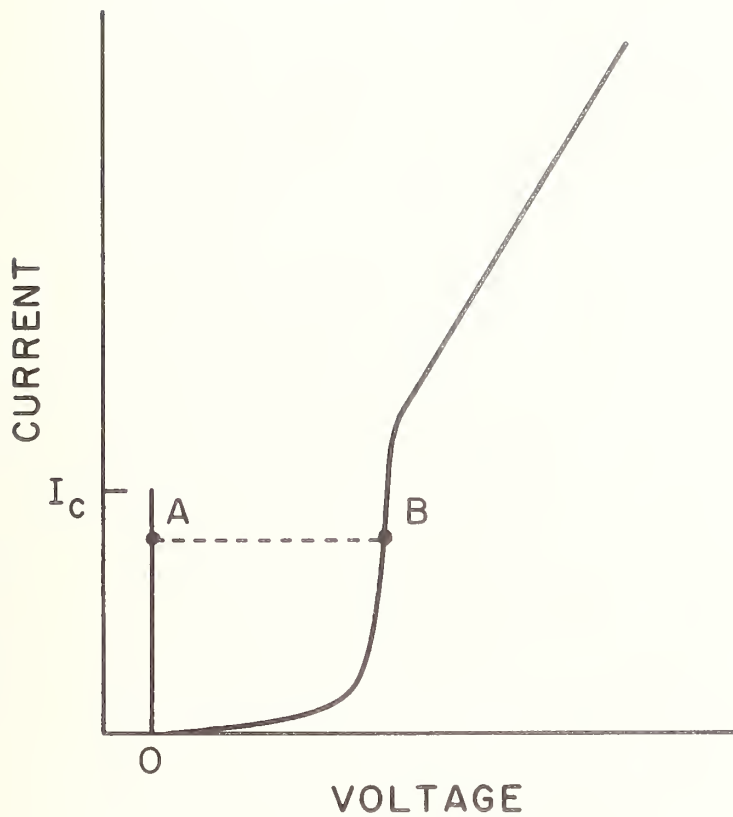


Figure 16. Current versus voltage characteristic of the gate of a tunneling cryotron. The operating points are marked A and B.

Another interesting achievement of these experimenters was to set up a very sensitive RF circuit to observe the influence of a passive resonant circuit on the I-V characteristic of a Josephson junction [27] (fig. 11). They were able to sense the presence of various resonant structures, including a sample of powdered cobalt inductively coupled to the circuit. They detected the nuclear magnetic resonance of  $\text{Co}^{59}$  at 218 MHz, showing that their instrument has potential as an RF spectrometer. Its distinctive feature in this respect is its very low level of excitation, which would be an advantage with a specimen with a very long relaxation time.

The current and voltage in an ideal Josephson junction at zero temperature would be related by

$$\frac{dI}{dt} = (2eV/\hbar) \cdot (I_c^2 - I^2)^{\frac{1}{2}}$$

when  $I \leq I_c$ , and this approximately represents the behavior of a real Josephson junction in experimentally accessible conditions. This relationship makes a Josephson junction an extremely efficient and broad band RF mixer, [58] with the additional feature that applying a DC bias adds the self-oscillation of the junction to the mix. The time dependence of the I-V relationship generates this and other unique properties not shared by classical non-linear mixers. We have already mentioned a demonstration of this effect at 0.2 Hz. At the other extreme, Kose, McDonald, Evenson, and Wells [59] have observed the mixing of signals from an HCN laser near 900 GHz by a Josephson junction.

The steps in the I-V characteristic of a Josephson junction under the influence of an RF signal are actually another manifestation of this mixing effect, with one of the resultant signals at zero frequency. Parker, Taylor, and Langenberg [60, 61] have measured the relationship between applied frequency  $f$  and voltage interval  $V$  for these steps to an accuracy

of a few parts per million. Assuming that the relationship truly is  $hf = 2eV$ , they used their results to derive a new value for the fine structure constant  $\alpha = e^2/\hbar c$ . This resolved an old discrepancy between the calculated and measured values of the hyperfine splitting of the hydrogen atom. It will probably have a significant impact on the accepted values of the fundamental constants.

They found the measured relationship between frequency and voltage to be independent of temperature within their experimental error. More recently Clarke<sup>[42]</sup> showed that this relationship is the same to one part in  $10^8$  in junctions made of lead, tin, and indium. This has raised the interesting possibility of ultimately using the Josephson effect to replace electrochemical cells to maintain the standard volt,<sup>[62]</sup> and there appear to be many potential advantages in doing so.

Another application related to RF mixing is the detection of radiation. Grimes, Richards, and Shapiro<sup>[63]</sup> have shown that when a point contact Josephson junction is biased to suitable operating point, it becomes a sensitive detector of long wavelength radiation. The usable range covers the radio and microwave regions of the spectrum, down to a short wavelength limit of a few hundred micrometers. Taking a detected bandwidth of 1 Hz, the minimum detectable signal is  $10^{-13}$  watts in a system sensitive to the whole spectrum or  $10^{-14}$  watts with a narrow band filter. In addition to this great sensitivity, the response time is very short ( $10^{-8}$  seconds), permitting high frequency chopping of the incident signal to discriminate against background radiation.

Finally, noise thermometry. Since the frequency of an oscillating Josephson junction is determined by the bias voltage, it follows that fluctuations in the voltage due to thermal noise will cause fluctuations in frequency. Measurement of these frequency fluctuations can therefore form the basis of a new scheme of absolute thermometry.<sup>[7]</sup> Once again, the

Josephson junction acts as a parametric up-converter which amplifies the very feeble noise voltage, generated by a resistor at a low temperature, to a high enough level to detect with a receiver at ambient temperature.

One technique to measure the frequency fluctuations is to use some kind of spectrum analyzer to measure the linewidth  $\Delta f$  of the oscillation. This is given by<sup>[10]</sup>

$$\Delta f = 16\pi e^2 k T R / h^2$$

assuming that the only source of noise is a resistor  $R$  at a temperature  $T$  connected in parallel with the junction. The quantity  $k$  is Boltzmann's constant. This relationship has been checked experimentally<sup>[17]</sup> in the range  $2 \text{ K} < T < 8 \text{ K}$ , and  $1.7 \times 10^{-10} \Omega < R < 2.6 \times 10^{-5} \Omega$ .

Another technique to measure the frequency fluctuations is directly with a frequency counter. Under the same assumptions as before the variance  $\langle (f - \langle f \rangle)^2 \rangle$  of fluctuations in repeated measurements of the frequency  $f$  with a counter with gate time  $\tau$  would be

$$\langle (f - \langle f \rangle)^2 \rangle = 8 e^2 k T R / \tau h^2.$$

Advantages of this technique are its facility for automation and the possibility of analyzing the statistics of the observed fluctuations to eliminate other sources of noise, such as flicker noise, with a different frequency spectrum.<sup>[19]</sup>

The interesting question is the low temperature limit of this scheme of thermometry. Assuming that extraneous sources of noise can be eliminated, the fundamental limit is set by photon shot noise generated by the Josephson junction.<sup>[15]</sup> This sets a lower limit of  $eV/k$  to the effective noise temperature of the junction. For a junction oscillating at 40 MHz this effective temperature would be  $10^{-3}$  K. It would be possible to measure lower temperatures if the resistor  $R$  were small compared to the

resistance of the junction. Thus the possibility exists of measuring absolute noise temperatures in the millikelvin range.

Looking back over the devices we have discussed, it appears that a Josephson junction is almost a universal sensor. This is a source of embarrassment when designing an experiment to measure a single quantity, but the rewards of perseverance are great.

## References

1. R. A. Kamper, L. O. Mullen, and D. B. Sullivan, Superconducting Thin Films, NASA Contractor Report CR 1189 (1968).
2. C. A. Neugebauer and R. A. Ekvall, Vapor-deposited superconductive films of Nb, Ta, and V, *J. Appl. Phys.* 35, 547-553 (1964).
3. B. W. Maxfield and W. L. McLean, Superconducting penetration depth of niobium, *Phys. Rev.* 139, A1515-1521 (1965).
4. W. DeSorbo, Effect of dissolved gases on some superconducting properties of niobium, *Phys. Rev.* 132, 107-121 (1963).
5. J. C. Swihart, Field solution for a thin-film superconducting strip transmission line, *J. Appl. Phys.* 32, 461-469 (1961).
6. J. E. Zimmerman, J. A. Cowen, and A. H. Silver, Coherent radiation from voltage-biased weakly connected superconductors, *Appl. Phys. Letters*, 9, 353-355 (1966).
7. R. A. Kamper, Millidegree noise thermometry, Symposium on the Physics of Superconducting Devices, Charlottesville, Virginia (ONR Report, 1967).
8. W. H. Louisell, *Coupled Mode and Parametric Electronics* (John Wiley and Sons, Inc., New York, N. Y., 1960).
9. J. M. Manley and H. E. Rowe, Some general properties of nonlinear elements - Part 1. General energy relations, *Proc. IRE* 44, 904-913 (1956).
10. R. E. Burgess, Quantization and fluctuations in superconductors, Symposium on the Physics of Superconducting Devices, Charlottesville, Virginia (ONR Report, 1967).
11. K. F. Knott, Measurement of battery noise and resistor-current noise at subaudio frequencies, *Electronics Letters* 1, 132 (1965).

12. D. J. Scalapino, Current fluctuations in superconducting tunnel junctions, Symposium on the Physics of Superconducting Devices, Charlottesville, Virginia (ONR Report, 1967).
13. Yu. M. Ivanchenko, Influence of quantum fluctuations on the width of the band of radiated frequencies in a superconducting tunnel structure, *ZhETF Pisma* 6, 879-881 (1967). Translation: *JETP Letters*, 6, 313-315 (1967).
14. A. I. Larkin and Yu. N. Ovchinnikov, Radiation line width in the Josephson effect, *Zh. Eksp. Teor. Fiz.*, 53, 2159-2163 (1967). Translation: *Soviet Physics JETP*, 26, 1219-1221 (1968).
15. M. J. Stephen, Theory of a Josephson oscillator, *Phys. Rev. Letters* 21, 1629-1632 (1968).
16. M. J. Stephen, Noise in the AC Josephson effect, *Phys. Rev.*, to be published.
17. A. H. Silver, J. E. Zimmerman, and R. A. Kamper, Contribution of thermal noise to the line-width of Josephson radiation from superconducting point contacts, *Appl. Phys. Letters*, 11, 209-211 (1967).
18. J. A. Barnes, Atomic timekeeping and the statistics of precision signal generators, *Proc. IEEE* 54, 207-220 (1966).
19. D. W. Allan, Statistics of atomic frequency standards, *Proc. IEEE* 54, 221-230 (1966).
20. F. Bloch, Nuclear induction, *Phys. Rev.* 70, 460-474 (1946).
21. E. R. Andrew, *Nuclear Magnetic Resonance* (Cambridge University Press, Cambridge, 1956).
22. F. N. H. Robinson, *Noise in Electrical Circuits* (Oxford University Press, London, 1962).
23. R. V. Pound and W. D. Knight, A radio frequency spectrograph and simple magnetic field meter, *Rev. Sci. Instr.* 21, 219-225 (1950).
24. F. N. H. Robinson, Nuclear resonance absorption circuit, *J. Sci. Instr.* 36, 481-487 (1959).

25. D. H. Howling, Signal and noise characteristics of the PKW marginal oscillator spectrometer, *Rev. Sci. Instr.* 36, 660-667 (1965); Signal and noise characteristics of the Robinson nuclear absorption circuit, *Rev. Sci. Instr.* 37, 891-892 (1966).
26. V. L. Newhouse and H. H. Edwards, An ultrasensitive linear cryotron amplifier, *Proc. IEEE* 52, 1191-1206 (1964).
27. A. H. Silver and J. E. Zimmerman, Multiple quantum resonance spectroscopy through weakly-connected superconductors, *Appl. Phys. Letters* 10, 142-145 (1967).
28. D. S. Miyoshi and R. M. Cotts, Helium cooled RF preamplifier for use in NMR, *Rev. Sci. Instr.* 39, 1881-1884 (1968).
29. D. W. Alderman, Nuclear Magnetic Resonance Study of KCl:Li<sup>+</sup> (Ph.D. thesis, Cornell University, 1969).
30. G. A. Persyn, J. M. Victor, and W. L. Rollwitz, High-Sensitivity Nuclear Magnetic Resonance for the Quantitative Analysis of Body Fluids (USAF School of Aerospace Medicine Report SAM-TR-67-70, 1967).
31. V. W. Hesterman, W. S. Goree, and F. Chilton, Review of Superconducting Magnetometers, (Stanford Research Institute Report, 1967).
32. B. S. Deaver and W. S. Goree, Some techniques for sensitive magnetic measurements using superconducting circuits and magnetic shields, *Rev. Sci. Instr.* 38, 311-318 (1967).
33. J. M. Pierce, A persistent current magnetometer with novel applications, Symposium on the Physics of Superconducting Devices, Charlottesville, Virginia (ONR Report, 1967).
34. J. E. Zimmerman and A. H. Silver, Macroscopic quantum interference effects through superconducting point contacts, *Phys. Rev.* 141, 367-375 (1966).

35. J. Clarke, The measurement of small voltages using a quantum interference device, Symposium on the Physics of Superconducting Devices, Charlottesville, Virginia (ONR Report, 1967).
36. J. E. Mercereau, Application of Quantum superconductivity to a new kind of instrumentation, *J. Appl. Phys.* 40, 1994 (1969) (Abstract only).
37. B. D. Josephson, Possible new effects in superconductive tunneling, *Physics Letters* 1, 251-253 (1962).
38. B. D. Josephson, Coupled superconductors, *Rev. Mod. Phys.* 36, 216-220 (1964).
39. B. D. Josephson, Supercurrents through barriers, *Adv. in Phys.* 14, 419-451 (1965).
40. P. W. Anderson and J. M. Rowell, Probable observation of the Josephson superconducting tunnel effect, *Phys. Rev. Letters* 10, 230-232 (1963).
41. I. Giaever, Energy gap in superconductors measured by electron tunneling, *Phys. Rev. Letters* 5, 147-148 (1960).
42. J. Clarke, Experimental comparison of the Josephson voltage-frequency relations in different superconductors, *Phys. Rev. Letters* 21, 1566-1569 (1968).
43. P. W. Anderson and A. H. Dayem, Radio-frequency effects in superconducting thin film bridges, *Phys. Rev. Letters* 13, 195-197 (1964).
44. D. E. McCumber, Effect of AC impedance on DC voltage-current characteristics of superconductor weak-link junctions, *J. Appl. Phys.* 39, 3113-3118 (1968).
45. W. C. Stewart, Current-voltage charactersitics of Josephson junctions, *Appl. Phys. Letters* 12, 277-280 (1968).

46. J. M. Rowell, Magnetic field dependence of the Josephson tunnel current, *Phys. Rev. Letters* 11, 200-202 (1963).
47. R. C. Jaklevic, J. Lambe, J. E. Mercereau, and A. H. Silver, Macroscopic quantum interference in superconductors, *Phys. Rev.* 140, A1628 - 1637 (1965).
48. R. E. Eck, D. J. Scalapino, and B. N. Taylor, Self-detection of the AC Josephson current, *Phys. Rev. Letters* 13, 15-18 (1964).
49. S. Shapiro, Josephson currents in superconducting tunneling: The effect of microwaves and other observations, *Phys. Rev. Letters* 11, 80-82 (1963).
50. D. N. Langenberg, D. J. Scalapino, B. N. Taylor, and R. E. Eck, Investigation of microwave radiation emitted by Josephson junctions, *Phys. Rev. Letters* 15, 294-297 (1965).
51. J. E. Zimmerman and A. H. Silver, A high-sensitivity superconducting detector. *J. Appl. Phys.* 39, 2679-2682 (1968).
52. D. N. Langenberg, D. J. Scalapino, and B. N. Taylor, Josephson-type superconducting tunnel junctions as generators of microwave and submillimeter wave radiation, *Proc. IEEE* 54, 560-575 (1966).
53. J. Clarke, A superconducting galvanometer employing Josephson tunneling, *Phil. Mag.* 13, 115-127 (1966).
54. R. Meservey, Proposed ammeter using flux quantization, *J. Appl. Phys.* 39, 2598-2605 (1968).
55. J. Matisoo, The tunneling cryotron - a superconductive logic element based on electron tunneling, *Proc. IEEE* 55, 172-180 (1967).
56. D. A. Buck, The cryotron - a superconductive computer component, *Proc. IRE* 44, 482-492 (1956).
57. J. M. Lock, Superconductive switching, *Reports on Progress in Physics* 25, 37-62 (1962).

58. C. C. Grimes and S. Shapiro, Millimeter-wave mixing with Josephson junctions, *Phys. Rev.* 169, 397-406 (1968).
59. V. E. Kose, D. B. McDonald, K. M. Evenson, and J. S. Wells, To be published.
60. D. N. Langenberg, W. H. Parker, and B. N. Taylor, Experimental test of the Josephson frequency-voltage relation, *Phys. Rev.* 150, 186-188 (1966).
61. W. H. Parker, B. N. Taylor, and D. N. Langenberg, Measurement of  $2e/h$  using the AC Josephson effect and its implications for quantum electrodynamics, *Phys. Rev. Letters* 18, 287-291 (1967).
62. B. N. Taylor, W. H. Parker, D. N. Langenberg, and A. Denenstein, On the use of the AC Josephson effect to maintain standards of electromotive force, *Metrologia* 3, 89-98 (1967).
63. C. C. Grimes, P. L. Richards, and S. Shapiro, Josephson effect far-infrared detector, *J. Appl. Phys.* 39, 3905-3912 (1968).



# NBS TECHNICAL PUBLICATIONS

## PERIODICALS

**JOURNAL OF RESEARCH** reports National Bureau of Standards research and development in physics, mathematics, chemistry, and engineering. Comprehensive scientific papers give complete details of the work, including laboratory data, experimental procedures, and theoretical and mathematical analyses. Illustrated with photographs, drawings, and charts.

*Published in three sections, available separately:*

### ● Physics and Chemistry

Papers of interest primarily to scientists working in these fields. This section covers a broad range of physical and chemical research, with major emphasis on standards of physical measurement, fundamental constants, and properties of matter. Issued six times a year. Annual subscription: Domestic, \$9.50; foreign, \$11.75\*.

### ● Mathematical Sciences

Studies and compilations designed mainly for the mathematician and theoretical physicist. Topics in mathematical statistics, theory of experiment design, numerical analysis, theoretical physics and chemistry, logical design and programming of computers and computer systems. Short numerical tables. Issued quarterly. Annual subscription: Domestic, \$5.00; foreign, \$6.25\*.

### ● Engineering and Instrumentation

Reporting results of interest chiefly to the engineer and the applied scientist. This section includes many of the new developments in instrumentation resulting from the Bureau's work in physical measurement, data processing, and development of test methods. It will also cover some of the work in acoustics, applied mechanics, building research, and cryogenic engineering. Issued quarterly. Annual subscription: Domestic, \$5.00; foreign, \$6.25\*.

## TECHNICAL NEWS BULLETIN

The best single source of information concerning the Bureau's research, developmental, cooperative and publication activities, this monthly publication is designed for the industry-oriented individual whose daily work involves intimate contact with science and technology—for engineers, chemists, physicists, research managers, product-development managers, and company executives. Annual subscription: Domestic, \$3.00; foreign, \$4.00\*.

\* Difference in price is due to extra cost of foreign mailing.

Order NBS publications from:

Superintendent of Documents  
Government Printing Office  
Washington, D.C. 20402

## NONPERIODICALS

**Applied Mathematics Series.** Mathematical tables, manuals, and studies.

**Building Science Series.** Research results, test methods, and performance criteria of building materials, components, systems, and structures.

**Handbooks.** Recommended codes of engineering and industrial practice (including safety codes) developed in cooperation with interested industries, professional organizations, and regulatory bodies.

**Special Publications.** Proceedings of NBS conferences, bibliographies, annual reports, wall charts, pamphlets, etc.

**Monographs.** Major contributions to the technical literature on various subjects related to the Bureau's scientific and technical activities.

**National Standard Reference Data Series.** NSRDS provides quantitative data on the physical and chemical properties of materials, compiled from the world's literature and critically evaluated.

**Product Standards.** Provide requirements for sizes, types, quality and methods for testing various industrial products. These standards are developed cooperatively with interested Government and industry groups and provide the basis for common understanding of product characteristics for both buyers and sellers. Their use is voluntary.

**Technical Notes.** This series consists of communications and reports (covering both other agency and NBS-sponsored work) of limited or transitory interest.

**Federal Information Processing Standards Publications.** This series is the official publication within the Federal Government for information on standards adopted and promulgated under the Public Law 89-306, and Bureau of the Budget Circular A-86 entitled, Standardization of Data Elements and Codes in Data Systems.

## CLEARINGHOUSE

The Clearinghouse for Federal Scientific and Technical Information, operated by NBS, supplies unclassified information related to Government-generated science and technology in defense, space, atomic energy, and other national programs. For further information on Clearinghouse services, write:

Clearinghouse  
U.S. Department of Commerce  
Springfield, Virginia 22151

U.S. DEPARTMENT OF COMMERCE  
WASHINGTON, D.C. 20230

OFFICIAL BUSINESS



POSTAGE AND FEES PAID  
U.S. DEPARTMENT OF COMMERCE

---